Unemployed Capital in Space*

Andrea Chiavari† Charles Cheng Zhang‡

August 7, 2024

This paper examines search-and-matching frictions in local capital markets. Leveraging a unique dataset we highlight a novel fact: spatial capital unemployment rate differences are persistent and mostly driven by different separation rates between capital and firms across locations. We show that a spatial search-and-matching model can fully account quantitatively for this observation. The social planner allocation does not coincide with the decentralized equilibrium and yields potentially sizeable welfare gains, providing a rationale for place-based policies.

Keywords: Local Capital Markets, Capital Unemployment, Search-and-Matching, Spatial Equilibrium, Place-Based Policies

JEL Codes: E20, E22, E60, R12, R13, R30, R33

*We thank Martin Ellison, Sergio de Ferra, Andrea Ferrero, Elisa Giannone, Alexandre N. Kohlhas, Pablo Ottonello, Barbara Petrongolo, Xincheng Qiu, Esteban Rossi-Hansberg, Edouard Schaal, Tony Venables, and Yanos Zylberberg as well as all the participants at Oxford for useful comments and suggestions.

†Department of Economics, University of Oxford. Email: andrea.chiavari@economics.ox.ac.uk

‡Department of Economics, University of Oxford. Email: cheng.zhang@economics.ox.ac.uk

1 Introduction

There is a consensus that capital accumulation plays a crucial role in local prosperity (Kleinman et al., 2023). There is also consensus from empirical studies on physical capital markets using micro-level data that the lengthy intervals between the supply of a capital unit and its absorption by demand are explained by trading frictions (Ramey and Shapiro, 2001; Gavazza, 2011). These trading frictions lead to significant capital unemployment—defined as idle units searching to be traded—at the aggregate level (Ottonello, 2021). A key question, then, is: How important is capital unemployment for local prosperity?

We address this question by integrating these two consensuses through a novel dataset that sheds light on local capital unemployment of structures. In doing so, we make three main contributions. First, our dataset reveals that capital unemployment differences are large and persistent, primarily driven by local differences in separation rates between firms and the capital they use. Second, we apply tools from spatial search-and-matching models of labor markets, demonstrating their versatility for local capital markets and their quantitative success in accounting for our empirical findings. Finally, we show that the model reveals an inefficient decentralized equilibrium, highlighting the potential for significant welfare gains from place-based policies.

Specifically, this study utilizes a *unique* panel dataset from Property Market Analysis (PMA) LLP, a global independent real estate research consultancy established in 1981. PMA's data is derived from a combination of secondary sources (national accounts, brokers, data providers) and in-depth primary research, which involves site visits and meetings with market participants. Spanning from 1981 to 2022, the dataset reports detailed spatial information on a widely used form of capital—structures—which represents more than 50 percent of the physical capital in the UK economy and covers 67 UK cities, contributing approximately 46 percent of the total UK GDP in 2021. It encompasses various real estate categories, including offices, industrial properties, and logistics facilities, providing data for each location and year. This dataset includes information on total capital stock (in thousands of square meters), the capital unemployment rate, and take-ups, representing the space becoming occupied in the year. Thus, this dataset offers an initial glimpse into the distribution of capital, both employed and unemployed, allowing for the study of how frictions in local capital markets influence the

spatial distribution and utilization of this factor of production. We assess and confirm the data quality by correlating our capital measure with official sources.

This dataset allows us to establish the following novel set of stylized facts on the spatial distribution of unemployed capital:

> **Fact 1:** Local capital unemployment rates are widely dispersed and highly persistent across locations in the UK.

> **Fact 2:** More prosperous locations exhibit lower local capital unemployment rates.

> **Fact 3:** The local capital investment rate is near the replacement rate level and does not seem to move to close the local capital unemployment rate gaps.

These large and persistent differences in the local capital unemployment rate cannot be easily explained by persistent shocks from deindustrialization, which might cause a mismatch between demand and supply in local capital markets. The importance of local prosperity in explaining these differences suggests long-term, steady-state economic forces are at play, as also supported by the fact that net investment rates in our data are near the replacement rate and do not seem to adjust to close these gaps.

To explore these long-run patterns, we employ a flow-based approach inspired by labor market methods (Shimer, 2012). This methodology uses reported observables from our dataset to infer unobservable probabilities for each location and period: the *finding rate*, representing the likelihood of unemployed capital becoming employed, and the *separation rate*, representing the likelihood of employed capital becoming unemployed. We find an average finding rate of 40 percent and an average separation rate of 3 percent. The high finding rate suggests that low local capital demand is unlikely to explain the large and persistent differences in capital unemployment rates. Additionally, this approach leads to a spatial decomposition, akin to Fujita and Ramey (2009) and Bilal (2023), linking capital unemployment rate differences to these rates. Applying this decomposition to our data reveals the following additional fact about the UK:

> **Fact 4:** Local capital unemployment rate gaps are mostly driven by differences in separation rates across locations.

Then, to understand the economic forces behind these patterns, we propose a search-and-matching model à la Pissarides (2000) of the capital market, with endogenous separation rates

as outlined in Den Haan et al. (2000). In the model, geographic locations differ in productivity. Given our focus on long-run steady-state dynamics, motivated by the data, capitalists—those owning the capital stock—and firms are allowed to move freely across locations. Capitalists with unemployed capital and firms with capital vacancies search for each other in local capital markets. Upon matching, an idiosyncratic match productivity is drawn, which then evolves stochastically over time. Matches dissolve when idiosyncratic productivity falls below an endogenous, location-specific threshold. The model's spatial equilibrium is sustained by differences in local costs of managing capital, similar in spirit to Rosen (1979)-Roback (1982).

Qualitatively, the model leads to two closed-form elasticities, generalizing Ljungqvist and Sargent (2017) fundamental surplus, which provide a simple explanation for all the empirical patterns we document. In highly productive locations, capital markets are tighter, i.e., they have high ratios of capital vacancies to unemployed capital, as firms benefit from higher profit flows in these areas. However, the spatial equilibrium condition limits the supply of capitalists with unemployed capital in these locations due to higher equilibrium costs of managing capital. Tighter capital markets result in longer durations for firms to fill capital vacancies, while unemployed capital finds firms more rapidly. With higher average productivity, fewer matches become unprofitable due to idiosyncratic productivity shocks, leading to lower separation rates. Consequently, lower separation rates and higher finding rates contribute to lower capital unemployment rates in areas with higher productivity.

To evaluate whether the model aligns with empirical observations quantitatively, we calibrate it by targeting finding and separation rates at the UK local capital market with a median capital unemployment rate, along with the capital unemployment rate differences between local capital markets with the highest and lowest capital unemployment rates. Subsequently, we gauge the model's quantitative performance by analyzing its performance on several untargeted moments such as GDP, the rental rate elasticity of local capital unemployment rate, and amenities. We find that the model performs satisfactorily on all these metrics.

We then assess the model's success by examining how spatial capital unemployment rates and the relative importance of finding and separation rates vary with productivity across locations. The model's calibration reveals a high profit rate for firms, leading to a high fundamental surplus, which in turn implies a small role for the finding rate. Our findings indicate that this simple model can quantitatively match all described facts, attributing 68 percent of

the contribution to spatial capital unemployment rate differences to the separation rate and 32 percent to the finding rate, closely aligning with our data.

Finally, we explore the social planner allocation of the economy, which implies a generalized Hosios (1990) condition, showing that the decentralized equilibrium is not necessarily efficient. The calibration indeed recovers a set of parameters that implies an inefficient allocation in which too many firms enter in equilibrium, making the local capital market excessively tight on the firm side. The planner aims to reduce the number of firms by redistributing a higher share of the surplus to capitalists via a higher rental capital rate. This increases the value of unemployed capital, but more so for high-productivity locations, implying a reallocation of capitalists to those locations, increasing the managing cost of capital in those locations. We find that welfare increases on average by 4 percent, with high-productivity locations losing some due to increased capital managing costs and low-productivity ones winning because of higher rental capital rates. We conclude by discussing how this social planner allocation provides a rationale for place-based policies that subsidize capitalists with unemployed capital, particularly in higher productivity locations. We also discuss the limitations of the model and how they might affect our normative conclusions.

Literature review. This paper contributes to several strands of the literature. First, this paper relates to Kleinman et al. (2023), who investigate dynamic capital accumulation in spatial general equilibrium settings. We complement their focus on a neoclassical investment model, where capital trading occurs in a Walrasian market, with a dynamic capital market framework grounded in search-and-matching frictions. Ample evidence from micro-level data on trading frictions in physical capital markets has been provided by Ramey and Shapiro (2001) and Gavazza (2011), among others.[1] This approach reveals the role of persistent capital unemployment rate differences in local prosperity and highlights the potentially substantial impact of place-based policies in generating welfare gains.

Second, it adds to the understanding of equilibrium unemployed capital, a topic initially explored by Ottonello (2021), who highlighted the significance of search frictions in explaining this phenomenon and its impact on business cycles. However, our focus differs as we investigate the role of capital unemployment rates and trading frictions for local prosperity and place-based policies.

[1]Evidence of friction in real estate markets have been also extensively documented, e.g., Genesove and Han (2012),Ngai and Tenreyro (2014), and Han and Strange (2015).

Finally, this paper relates to studies by Kline and Moretti (2013), Şahin et al. (2014), Marinescu and Rathelot (2018), Schmutz and Sidibé (2019), Kuhn et al. (2021), Bilal (2023), and Jung et al. (2023), which explore spatial variants of the Diamond (1982), Mortensen (1982), and Pissarides (1985) models embedded in spatial equilibrium frameworks like Rosen (1979) and Roback (1982).[2] Our paper complements this literature by demonstrating that insights from spatial search-and-matching models of local labor markets can be extended to local capital markets, explaining novel facts about the persistence of capital unemployment rate spatial gaps. Moreover, our empirical findings echo those of Kuhn et al. (2021) and Bilal (2023) for local labor markets, highlighting that persistent differences in separation rates are the main drivers of persistent capital unemployment rate spatial gaps.

Outline. Section 2 introduces our dataset. Section 3 details our stylized facts. Section 4 introduces the model, while Section 5 provides a quantitative assessment and the normative analysis. Finally, Section 6 offers concluding remarks.

2 Data

This section outlines the data and subsequently illustrates the spatial distribution and persistence of total and unemployed capital stock.

2.1 Description of the Main Data

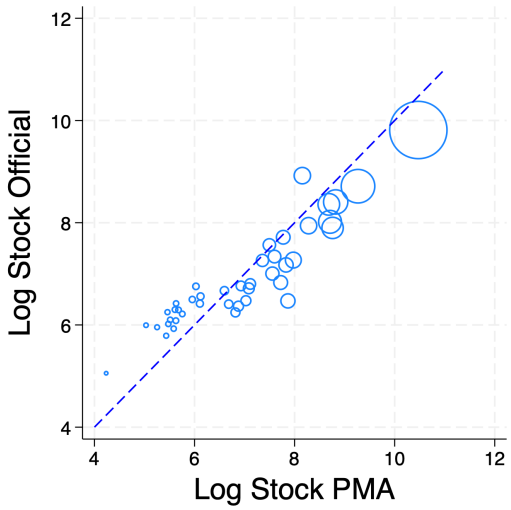
Understanding the dynamics of capital transitioning between being employed and unemployed is crucial for assessing its utilization in an economy. While time series data highlights variations in capital unemployment rates over time (Ottonello, 2021), spatial information is limited. This scarcity is due to the absence of detailed geographical data on capital, often available only at a high level of aggregation, and the lack of data sources offering insights into the spatial distribution and flows of unemployed capital.

This study utilizes panel data from Property Market Analysis (PMA) LLP, a global independent real estate research consultancy established in 1981, serving private sector entities, including real estate companies (JLL, Knight Frank, CBRE, Savills), financial institutions (Black-

[2]This study, along with many of the studies cited above, also belongs to the literature emphasizing spatial persistence, which is extensive in scope. This literature review does not aim to fully do justice to the many important papers that have contributed to it; for a recent review, see Allen and Donaldson (2022).

Rock, AIG), sovereign wealth funds (The Crown Estate, GIC, Temasek), and banks (Barclays, UBS, BNP Paribas). The dataset reports detailed spatial information on a widely used form of capital—structures—which represents more than 50 percent of the physical capital in the UK economy.[3] Analysts at PMA gather and scrutinize data from various secondary sources like national accounts, brokers, and data providers. They complement this with thorough primary research, including on-site visits and engagements with key market stakeholders.

Figure 1: Official vs. PMA Capital Stock



Note: Figure 1 depicts the spatial correlation between time-averaged log capital stocks from our dataset and official sources. Both measures are in thousands of square meters. Circle size represents each UK location's relative size.

The dataset, covering 1981 to 2022, encompasses 67 UK cities, contributing about 46 percent to the total UK GDP in 2021, and several European cities.[4] This paper primarily uses UK data from 1990 due to its extensive coverage and data quality, with European data serving as a secondary source for validation. The dataset spans several real estate categories—offices, industrial properties, and logistics facilities—providing information for each location and year, including total capital stock (in thousands of square meters), the capital unemployment rate, and take-ups, indicating the space taken up in the year.[5]

[3]Buildings and structures constitute between 48 to 68 percent of total physical capital, which is defined as buildings and structures plus equipment. These numbers are based on the author's own calculations using nationally representative ONS data.

[4]Included European cities: Amsterdam, Antwerp, Barcelona, Berlin, Brussels, Budapest, Cologne, Copenhagen, Dublin, Dusseldorf, Frankfurt, Hamburg, Helsinki, Lille, Lisbon, Luxembourg, Lyon, Madrid, Marseille, Milan, Oslo, Paris, Prague, Rome, Rotterdam, Stockholm, Stuttgart, Vienna, and Warsaw.

[5]PMA takes regular care to check that its capital measure contains only viable structures. Capital unemployment rate followed the standard definition used for labor unemployment rate and is measured as those viable

We gauge data quality by correlating our capital measure with official sources (Figure 1). The official capital stock data is obtained from the *Energy Performance of Buildings* project, initiated by the Department for Levelling Up, Housing & Communities. This project collects information, including floor area, for most commercial real estate buildings. We aggregate the floor area by city to estimate the capital stock at the city level. A robust spatial correlation between this official source and our measure suggests the reliability of our data. Additional details on data cleaning and validation exercises are provided in Appendices A.1 and A.2.

2.2 Additional Data Sources

We complement the PMA data with information from the ONS. Local output by industry is obtained from the *Regional Gross Value Added (Balanced) by Industry: All ITL Regions* dataset, which is used to calculate local labor and capital productivity, as well as measures of local exposure to persistent deindustrialization shocks. Measures of local population density are obtained by combining the *Population Profiles for Local Authorities* dataset and area information from the *Open Geography Portal*. Additionally, we obtain crime rates and health indices—two supplementary measures of local prosperity used in our analysis—from the *Recorded Crime Data by Community Safety Partnership Area* dataset and the *Health Index Scores* dataset, respectively. Finally, local labor unemployment rates are sourced from the *Regional Labour Market: Local Indicators for ITL3 Geography* dataset.

3 Empirical Analysis

This section explores the spatial patterns of local capital unemployment rates, establishing four main facts.

3.1 Distribution and Spatial Persistence of Capital Unemployment Rates

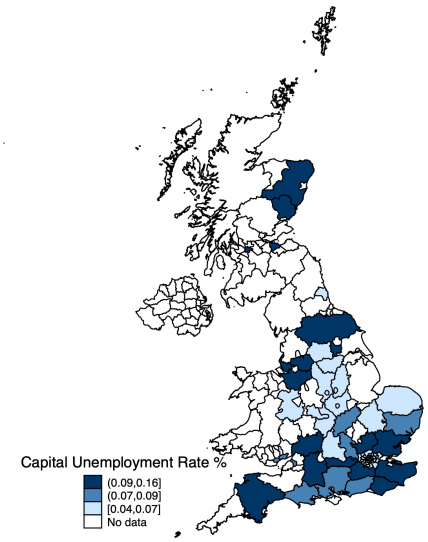
This section explores the spatial distribution and persistence of local capital unemployment rates in the UK, establishing three regularities.

structures on the market but not yet occupied.

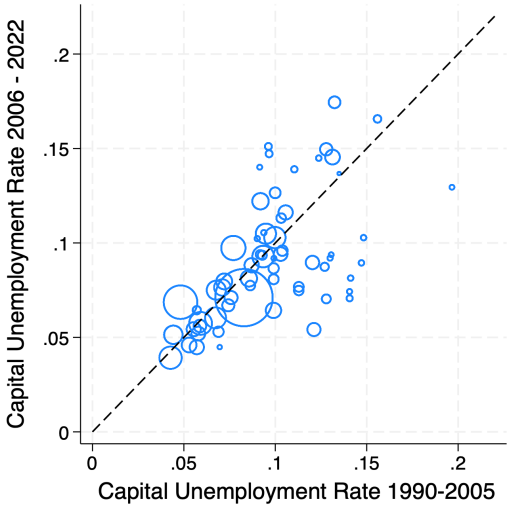
Fact 1: *Local capital unemployment rates are widely dispersed and highly persistent across locations in UK.*

Figure 2 shows this point. Figure 2a displays the capital unemployment rate across UK cities, where darker shades of blue represent higher rates. The data highlights substantial differences among cities, with unemployment rates of capital ranging on average from 4 to 16 percent. To assess the persistence of local capital unemployment rates, we divide the sample into two subperiods, pre and post-2006. Figure 2b plots the local capital unemployment rate in the second subperiod against the local capital unemployment rate in the first subperiod for every UK city. The local capital unemployment rates across UK cities exhibit notable persistence, aligning closely around the dashed black 45-degree reference line. This visual inspection is confirmed by a weighted autocorrelation coefficient across the two subperiods of 0.89.

Figure 2: Spatial Distribution and Persistence of Capital Unemployment Rate



(a) Local Capital Unemployment Rate



(b) Persistence of Capital Unemployment Rate

Note: Figure 2 provides an overview of the spatial distribution and persistence of the capital unemployment rate in cities across the UK. Figure 2a maps capital unemployment rates in UK cities based on the PMA dataset. Figure 2b plots capital unemployment rates in UK cities in two subperiods of the sample. The blue circles represent cities in the UK, and the size of each circle corresponds to the total capital within that city.

Appendix A.3 presents additional evidence that complements our findings using binscatter plots of capital unemployment rates, documenting the strong persistence of these patterns across different time horizons. Furthermore, Appendix A.3 extends this analysis to European

cities, confirming the observed patterns.

One potential factor behind Fact 1 is persistent shocks, which generate a potential mismatch between the existing local supply of capital and the changing demand due to the evolving local sectoral composition, driven by the deindustrialization process experienced by the UK (Kitson and Michie, 2014; Rice and Venables, 2021). In Appendix A.3, we show that controlling for this, by netting out the contribution of time fixed effects or the location-specific exposure to economy-wide industry cycles from local capital unemployment rates, yields a similar picture to Figure 2. Thus, we conclude that persistent deindustrialization shocks do not seem enough to fully explain our findings. One plausible explanation for this finding is that our dataset, with a large fraction of offices, consists of properties that are highly substitutable across different sectors. As a result, they are not significantly affected by changing demand due to shifting sectoral composition. In search of plausible predictors of existing local capital unemployment rate gaps, we introduce our next observation.

Fact 2: *More prosperous locations exhibit lower local capital unemployment rates.*

Table 1 shows this point. In particular, it correlates the local capital unemployment rate with several observables related to the prosperity of the location, controlling for city and time-fixed effects, city-specific quadratic trends, capital composition, industry mix, and investment dynamics.[6,7] The measures of prosperity considered in the analysis are labor productivity, measured as value-added to population; capital productivity, measured as value-added to total capital; density, measured as population per meter square; crime rate per capita and health index; and local labor unemployment rate. Standard errors are clustered at the city level to account for spatial serial correlation.

Columns (1) to (5) in Table 1 clearly show that more prosperous locations have a lower capital unemployment rate. In particular, locations with higher labor and capital productivity or higher density exhibit a lower capital unemployment rate. A higher crime rate per capita is associated with high capital unemployment rate levels, while a higher health index predicts

[6]Controlling for the capital composition means that we control for the share of industry-related and logistics-related structures as a share of total structures. To control for the industry mix in a given city, we control for the share of value-added accounted for by the manufacturing sector.

[7]We use a linear time trend instead of quadratic when using the crime rate per capita and the health index because of the low number of observations.

Table 1: Capital Unemployment Rate and Its Correlates

Dependent Variable	Capital Unemployment Rate							
	(1)	(2)	(3)	(4)	(5)	(6)	(7)	(8)
Labor Productivity	-0.224**							
	(0.133)							
Capital Productivity		-0.236***						
		(0.069)						
Density			-0.824^{+}					
			(0.522)					
Others								
Crime Rate Per Capita				0.499***				
				(0.000)				
Health Index				-0.564***				
				(0.000)				
Labor Unemployment Rate					0.929			
					(0.956)			
Capital Mix								
Industrial Property Share						-0.065**		
						(0.031)		
Logistics Facilities Share						-0.065		
						(0.056)		
Manufacturing Share							-0.069	
							(0.118)	
Net Investment Rate								0.034
								(0.105)
Fixed Effects								
City	✓	✓	✓	✓	✓	✓	✓	✓
Time	✓	✓	✓	✓	✓	✓	✓	✓
Controlls								
City-specific Time Trend	✓	✓	✓	✓	✓	✓	✓	✓
Others	✓	✓	✓	✓	✓	✗	✗	✗
Observations	487	487	476	44	487	986	487	558

Note. Labor productivity, capital productivity, density, and health index are in logs, the other independent variables are ratios. City-specific time trends are quadratic, except for column 4, where they are linear due to the insufficient number of observations to estimate higher-order trends. Other controls include the capital mix, manufacturing share, and net investment. Standard errors are clustered at the city level and reported in parentheses. $^{+}$,*, **, and *** denote 15, 10, 5, and 1% statistical significance respectively.

lower levels. Finally, albeit not statistically significant, a higher labor unemployment rate predicts a higher capital unemployment rate.

Moreover, columns (5) to (7) show how local capital unemployment rates correlate with local capital and industry mix. Locations with high industrial properties or logistic facilities as a share of total capital exhibit lower capital unemployment rates, albeit this is not always statistically significant. Moreover, a high manufacturing share of value-added does not seem associated with particular capital unemployment rate levels. This helps to understand why before we did not find a strong effect of measured deindustrialization shocks on local capital

unemployment rate dispersion and persistence. If deindustrialization were the main driver of differences in the local capital unemployment rate, we would expect cities with many manufacturing buildings to face depressed demand for these facilities. Consequently, localities with a high number of industrial and logistics buildings, or a high share of manufacturing activities, would be associated with a higher local capital unemployment rate. However, this does not seem to be the case in our data. Appendix A.3.3 shows that these results are robust to using alternative measures of the location-specific exposure to economy-wide industry cycles.

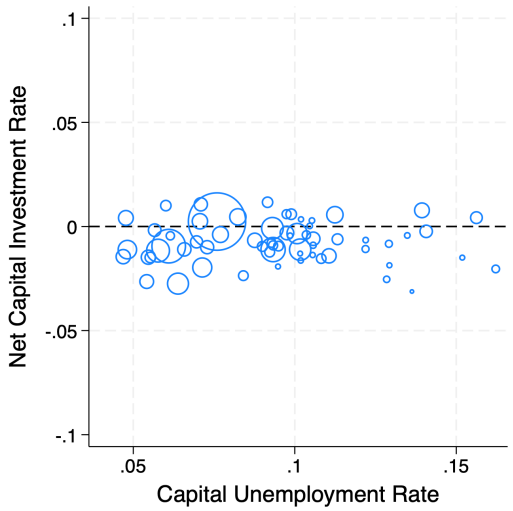
Finally, column (8) shows that the correlation between the net investment rate, i.e., the growth rate of capital, and the local capital unemployment rate is almost zero and statistically insignificant, which introduces our third empirical observation.

Fact 3: *The local capital investment rate is near the replacement rate level and does not seem to move to close the local capital unemployment rate gaps.*

Figure 3 presents the average net investment rate across UK cities sorted by local capital unemployment rate. There is no pattern of net investment rates moving to close local capital unemployment rate gaps. The correlation is close to zero as already documented in column (8) of Table 1. Moreover, we observe that in our data the average net investment rate is approximately zero with more than fifty cities having a net investment zero below 1 percent. Since, by definition investment rate equals the net investment rate plus the depreciation rate, we conclude that most local investment is close to depreciation, i.e., at the replacement rate.

Taking stocks, we find that local capital unemployment rate differences are large and persistent (Fact 1). None of these two observations are easily accountable for by persistent shocks triggered by deindustrialization forces potentially generating a mismatch between demand and supply in local capital markets. If anything, we find that most of these differences are highly associated with measures of local prosperity (Fact 2). This seems to suggest that explanations behind these spatial differences must be searched in long-run, steady-state-like, economic forces. Consistently with this interpretation, we find that net investment rates are near the replacement rate in our data, and do not seem to move to close these gaps (Fact 3). In search of these long-run forces shaping persistent differences in local capital unemployment rates, in the next section, we zoom on the flows in and out of capital unemployment,

Figure 3: Local Net Investment Rates



Note: Figure 3 provides an overview of average local net investment rates across UK cities. The blue circles represent cities in the UK, and the size of each circle corresponds to the total capital within that city.

establishing our fourth fact.

3.2 The Spatial Ins and Outs of Unemployed Capital

This section introduces a flow-based approach to understanding unemployed capital rate differences and establishes our fourth fact.

3.2.1 Flow-Based Approach to Unemployed Capital. Here, we introduce a flow-based approach, akin to the labor market approach in Shimer (2012) and Bilal (2023), to understand the spatial distribution of unemployed capital.

Time is discrete and indexed by t, locations by j. Observable variables are in bold. Specifically, $\boldsymbol{K}_{jt}$ is the total capital stock; $\boldsymbol{K}^u_{jt}$ is unemployed capital, obtained by multiplying the total stock by the unemployment rate; $\boldsymbol{K}^e_{jt}$ is employed capital, i.e., the difference between total stock and unemployed capital; and $\boldsymbol{M}_{jt}$ denotes the capital transitioning into employment.

The law of motion of total capital stock is given by:

$$\boldsymbol{K}_{jt} = (1-\delta)\boldsymbol{K}_{jt-1} + X_{jt-1}, \tag{1}$$

where δ is the depreciation rate and X_{jt-1} is total investment. In line with BEA calculations

for structures, we use a depreciation rate of 2 percent.[8] The law of motions of total employed and unemployed capital is given by:

$$\boldsymbol{K}^{e}_{jt} = f_{jt}[(1-\delta)\boldsymbol{K}^{u}_{jt-1} + X_{jt-1}] + (1-s_{jt})(1-\delta)\boldsymbol{K}^{e}_{jt-1}, \tag{2}$$

$$\boldsymbol{K}^{u}_{jt} = (1-f_{jt})[(1-\delta)\boldsymbol{K}^{u}_{jt-1} + X_{jt-1}] + s_{jt}(1-\delta)\boldsymbol{K}^{e}_{jt-1}; \tag{3}$$

where f_{jt} denotes the probability of unemployed capital becoming employed, which we refer to as "finding rate," while s_{jt} is the probability of employed capital becoming unemployed, which we refer to as "separation rate." Equation (2) assumes that newly invested capital starts as unemployed.

The total amount of unemployed capital that is taken up in a given period is given by:

$$\boldsymbol{M}_{jt} = f_{jt}[(1-\delta)\boldsymbol{K}^{u}_{jt-1} + X_{jt-1}], \tag{4}$$

i.e., the probability that unemployed capital becomes employed times the total stock of unemployed capital that carries over from the previous period.

Equations (1), (2), (3), and (4) can be employed to describe total investment X_{jt}, the finding rate f_{jt}, and the separation rate s_{jt} as functions of observables and parameters denoted by:

$$X_{jt} = \boldsymbol{K}_{jt+1} - (1-\delta)\boldsymbol{K}_{jt}, \tag{5}$$

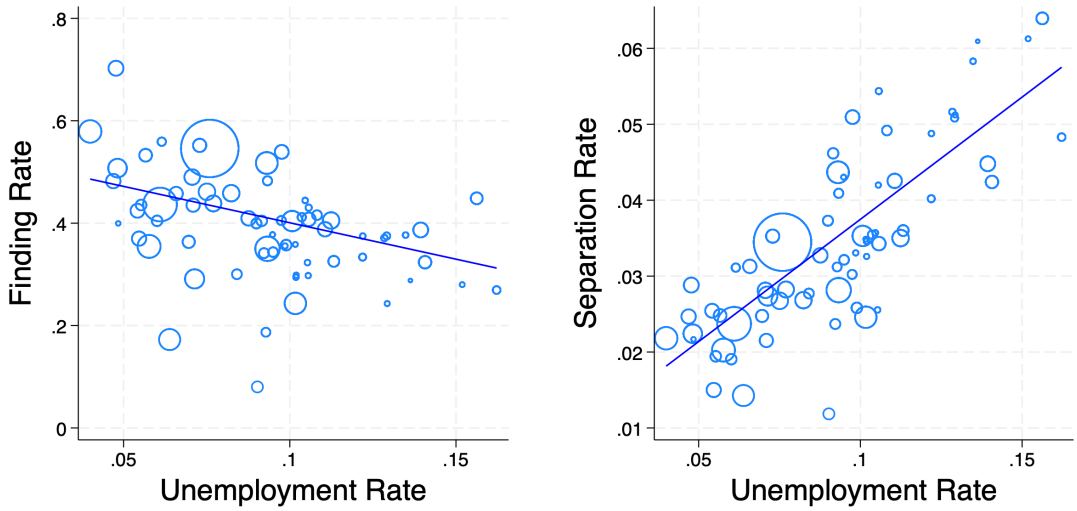
$$f_{jt} = \boldsymbol{M}_{jt}/[(1-\delta)\boldsymbol{K}^{u}_{jt-1} + X_{jt-1}], \tag{6}$$

$$s_{jt} = \{\boldsymbol{M}_{jt} - [\boldsymbol{K}^{e}_{jt} - (1-\delta)\boldsymbol{K}^{e}_{jt-1}]\}/[(1-\delta)\boldsymbol{K}^{e}_{jt-1}]. \tag{7}$$

Figure 4 shows the relation between the local capital unemployment rate and the finding and separation rates. The median finding rate is 40 percent (Figure 4a) while the median separation rate is 3 percent (Figure 4b). Overall, high finding rates in local capital markets are consistent with substantial demand for these structures, explaining why low demand or mismatch explanations associated with persistent deindustrialization shocks did not seem to have a major bite in the previous section.

[8] Sourse: BEA Depreciation Rates.

Figure 4: Capital Market Flows Across Space



(a) Finding Rate **(b) Separation Rate**

Note: Figure 4 shows the finding rate and the separation rate across different UK local capital markets sorted by their capital unemployment rate. Figure 4a displays the finding rate against the capital unemployment rate, across cities in the UK. Figure 4b displays the separation rate against the capital unemployment rate, across cities in the UK, across cities in the UK. Open blue circles represent cities in the UK, with size proportional to their total capital. Each data point represents a within-city average. The straight line in blue represents the best fit.

Finally, we can derive the following steady-state relation for $\delta \approx 0$ using equation (3):

$$\log\left(\frac{\boldsymbol{k}_j^u}{\boldsymbol{k}_j^e}\right) \approx \log(s_j) - \log(f_j), \tag{8}$$

where $\boldsymbol{k}_j^u$ is the capital unemployment rate and $\boldsymbol{k}_j^e$ is the employment capital rate. Equation (8) states that the log of the unemployment-employment capital rate ratio equals the log of the separation rate net of the log of the finding rate. Appendix A.4.2 generalizes equation (8) to any value of δ, showing that this approximation does not affect our conclusions.

From equation (8), we arrive at a spatial application of the unemployment decomposition formula (e.g., Fujita and Ramey, 2009), given by:

$$\mathbb{V}\left(\log\left(\frac{\boldsymbol{k}_j^u}{\boldsymbol{k}_j^e}\right)\right) = \mathbb{C}\left(\log\left(\frac{\boldsymbol{k}_j^u}{\boldsymbol{k}_j^e}\right), \log(s_j)\right) + \mathbb{C}\left(\log\left(\frac{\boldsymbol{k}_j^u}{\boldsymbol{k}_j^e}\right), -\log(f_j)\right) + \varepsilon_j. \tag{9}$$

Equation (9) systematically breaks down the impact of each component in equation (8), i.e., separation and finding rates, on the variance of the log of the unemployment-employment capital rate ratio. Additionally, it allows for an error wedge ε_j, which may result both from

measurement error in the data or departures from the steady-state assumption imposed above.[9]

3.2.2 Descriptive Findings. In this section, we depict the contribution of separation rates and finding rates to the local capital unemployment rate using equation (8).

Fact 4: *Local capital unemployment rate gaps are mostly driven by differences in separation rates across locations.*

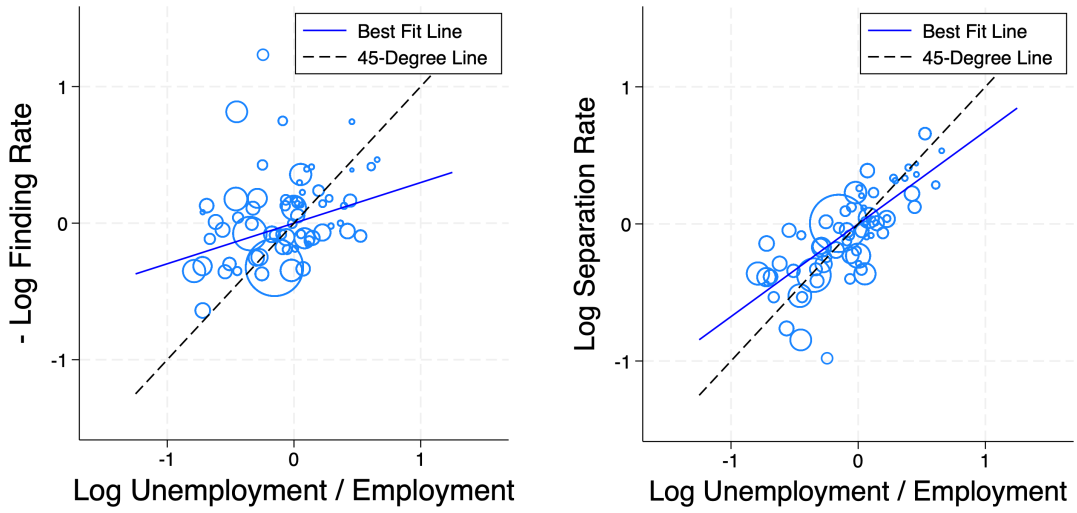
Figure 8 plots minus the log of finding rates f_j and the log of separation rates s_j against the log of the unemployment-employment capital rate ratio $\boldsymbol{k}_j^u/\boldsymbol{k}_j^e$ across cities in the UK. Figure 8a shows that finding rates exhibit low variation across locations, with the best-fit line notably distant from the 45-degree line (dashed black line). In contrast, separation rates are the main factor driving differences in local capital unemployment rates, as indicated in Figure 8b. Separation rates vary substantially across locations, and their best-fit line closely aligns with the 45-degree line.

Quantitatively, our analysis, using equation (9) for a precise variance decomposition, reveals that in the UK, the separation rate accounts for 68 percent of the cross-sectional variation in spatial capital unemployment rates. Finding rates contribute 30 percent of the variation. With the remaining 2 percent attributable to the error wedge. This leads us to conclude that neither measurement error nor the steady-state assumption is particularly demanding in our setting. The latter supports the conclusion on steady-state-like behavior from Section 3.1.

We confirm the robustness of our findings through additional exercises. Appendix A.4.1 demonstrates that the importance of separation rates in driving differences in local unemployment rates is not unique to the UK; it holds for European cities as well. Finally, expanding equation (8) to accommodate δ greater than zero enables us to consider the contribution of the extensive margin from newly invested capital. Appendix A.4.2 demonstrates that this extended decomposition reaffirms the predominant role of the separation rate, revealing a limited role for the extensive margin. These conclusions hold for both the UK and the European context.

[9] In principle it could arise also form the assumption of $\delta \approx 0$. However, we generalize equation (8) to any value of δ in Appendix A.4.2, showing that this approximation does not matter significantly for our results.

Figure 5: Capital Market Flows Decomposition Across Space



(a) Finding Rate **(b) Separation Rate**

Note: Figure 4 shows graphically the contribution of minus the log of the finding rate and the log of the separation rate to local capital unemployment rate differences across UK locations. Figure 4a scatterplots minus the log of the finding rate against the log of the unemployment-employment capital ratio, across cities in the UK. Figure 4b scatterplots the log of the separation rate against the log of the unemployment-employment capital ratio, across cities in the UK. Open blue circles represent cities in the UK, with size proportional to their total capital. Each data point represents a within-city average, with cross-sectional means removed for the plot. The 45-degree line is in dashed black.

4 Model

This section presents the model of local capital markets used in the paper to study the long-run spatial distribution of capital unemployment rate gaps, unveils the economic forces driving the contribution of different capital flows to their persistence, and investigates its efficiency properties.

4.1 Primitives, Timing, and Capital Markets

Time is discrete and indexed by t.[10] There are J local capital markets indexed by $j = \{1, \ldots, J\}$. At each location j, there is a mass K_j of infinitely lived, risk-neutral capitalists owning one unit of capital, along with a mass of profit-maximizing firms. Both capitalists and firms are *ex-ante* homogeneous, sharing a common discount factor β. Each location j is characterized by its amenities A_j, fundamental productivity Z_j, and local cost of managing capital $g'(K_j) \equiv g'_j$,

[10] Given our focus on the steady-state equilibrium, as motivated by Figure 2b, we largely omit the t subscript.

which is twice differentiable and convex and captures congestion externalities arising from placing all the capital in the same location.[11]

A capitalist's capital unit is either rented, making it employed, or not, remaining unemployed. Each capitalist incurs the local cost of managing the capital, and those renting their capital receive a local rental rate. On the other side of the market, firms have free entry and can choose where to search for capital at a per-period cost κ. Firms operate with constant returns to scale technologies, leaving firm size undetermined, and we consider one capital unit-firm match.

We build on the extensive real estate literature emphasizing the presence of search frictions in these markets (e.g., Genesove and Han, 2012; Ngai and Tenreyro, 2014; Han and Strange, 2015), as well as on the literature emphasizing trading frictions and long times between the moment a unit of capital is listed and the time it is sold (e.g., Ramey and Shapiro, 1998; Gavazza, 2011; Ottonello, 2021) to motivate the microstructure of our local capital markets.[12] In particular, we assume that contacts between capitalists and firms follow a constant-returns-to-scale matching function $M(K_j^u, V_j^k)$ in each local capital market, where K_j^u is unemployed capital and V_j^k is the capital vacancies in market j. Using lowercase letters for rates normalized by total capital, k_j^u is the unemployment rate, and v_j^k is the capital vacancy rate. Capital market tightness is denoted by $\theta_j = v_j^k/k_j^u$. The contact rate for searching capitalists is $p(\theta_j) = M(1, \theta_j)$, and for searching firms, it is $q(\theta_j) = M(\theta_j^{-1}, 1)$, with $p(\theta_j) = \theta_j q(\theta_j)$.

Each capitalist-firm match yields period output $y_j(z) = Z_j z$, determined by the location-specific fundamental productivity Z_j and an i.i.d. match-specific stochastic productivity z with distribution $F(z)$. Producing firms must also incur a fixed cost c associated with operating the production technology. Idiosyncratic productivity shocks are realized, and each capitalist-firm match decides whether to continue the match in the next period. Upon separation, the capitalists' capital enters the next period as unemployed. Additionally, matches are destroyed exogenously with probability d, and capital depreciates at rate δ, being replaced one-to-one by new capital starting as unemployed. Rental rates, $r_j(z)$, are determined through state-contingent generalized Nash bargaining, where capitalists have bargain-

[11] Interpreting g_j' as the local cost of managing capital implies leaving capitalists' location choice indeterminate, i.e., allowing them to live in a location potentially different from where they place their capital. This local managing cost can be microfounded by a competitive real estate servicing market, where g_j' represents the marginal cost of supplying services to the local capitalists K_j.

[12] Plenty of anecdotal evidence supports the presence of search frictions in local commercial real estate markets, as described by the *National Association of Realtors*.

ing power $\eta \in (0,1)$.

The model timing is as follows: period t comprises two stages, A and B. In stage A, unemployed capitalists search, then exogenous separations d realize. Subsequently, firms decide whether to maintain the match once the shock z is realized. In stage B, production occurs, followed by capital depreciation with probability δ. Value functions are written in stage B.

4.2 Local Capital Market Equilibrium

The value functions for capitalists with unemployed and employed capital in the local capital market j have the following recursive representation:

$$V_j^u = -\ell_j + (1-\delta)\beta \left\{ V_j^u + p(\theta_j)(1-d)\mathbb{E}[V_j^e(z') - V_j^u]^+ \right\}, \tag{10}$$

$$V_j^e(z) = r_j(z) - \ell_j + (1-\delta)\beta \left\{ V_j^u + (1-d)\mathbb{E}[V_j^e(z') - V_j^u]^+ \right\}; \tag{11}$$

where $\ell_j \equiv -A_j + g_j'$ denotes the effective cost of managing capital, and $\mathbb{E}[\cdot]^+$ denotes the expectation over the $\max\{\cdot, 0\}$ with respect to future productivity z'. This operator over continuation values represents the optimal separation decision.

The value of a matched firm and a firm with a capital vacancy in the local capital market j have the following recursive representations:

$$V_j^p(z) = y_j(z) - c - r_j(z) + (1-\delta)\beta(1-d)\mathbb{E}[V_j^p(z') - V_j^v]^+, \tag{12}$$

$$V_j^v = -\kappa + (1-\delta)\beta q(\theta_j)(1-d)\mathbb{E}[V_j^p(z') - V_j^v]^+. \tag{13}$$

As firms can freely choose which local capital market j to enter, the value of a firm with a capital vacancy must be zero in equilibrium, leading to the following free-entry condition:

$$\kappa = (1-\delta)\beta q(\theta_j)(1-d)\mathbb{E}[V_j^p(z')]^+, \tag{14}$$

saying that the cost of posting capital vacancies must equalize the expected value of producing with that unit of capital. As anticipated in Section 4.1, we follow the literature and assume that total surplus, denoted as $V_j^e(z) - V_j^u + V_j^p(z)$, is split between capital owners and firms according to a Nash bargaining protocol, with η representing the capital owners' bargaining

power. In this protocol, the capital owners' surplus, $V_j^e(z) - V_j^u$, equals a fraction η of the total surplus, while the firm surplus, $V_j^p(z)$, equals the $1-\eta$ remaining fraction. The rental rate for capital that achieves this split, as shown in Appendix B.1, is given by:

$$r_j(z) = \eta \left(y_j(z) - c + \kappa \theta_j \right). \tag{15}$$

Combining equations (12), (14), and (15) yields:

$$V_j^p(z) = (1-\eta)(y_j(z) - c) - \eta \kappa \theta_j + \frac{\kappa}{q(\theta_j)}. \tag{16}$$

Capitalist-firm matches are sustained as long as they yield a weekly positive production value for the firm, leading to the following threshold level z_j^R:

$$0 = (1-\eta)(y_j(z_j^R) - c) - \eta \kappa \theta_j + \frac{\kappa}{q(\theta_j)}. \tag{17}$$

Individual local capital markets are described by a Diamond-Mortensen-Pissarides model with endogenous separations, the definition of within-location equilibrium is standard (Pissarides, 2000) and characterized by equations (14), (16), and (17). The key condition is free entry into capital vacancy creation which implies that there are zero profits from posting a capital vacancy in each market, making firms indifferent between posting vacancies in different local capital markets. The resulting separation rate s and finding rate f are as follows:

$$s_j = 1 - (1-d)\left(1 - F(z_j^R)\right), \tag{18}$$

$$f_j = p(\theta_j)(1-d)\left(1 - F(z_j^R)\right); \tag{19}$$

where $1-d$ is the exogenous match survival probability, $1 - F(z_j^R)$ is the endogenous match survival probability, and $p(\theta_j)$ is the contact rate for searching capitalists. Equations (18) and (19) show that the model must exhibit low elasticity of market tightness θ_j to location-specific productivity and high elasticity of the separation threshold level z_j^R to location-specific productivity to successfully explain the findings in Section 3, particularly the predominant role of separation rates in explaining capital unemployment rate gaps across locations. The next section explores the conditions under which this is possible.

4.3 Inspecting the Mechanism

This section characterizes the fundamental elasticities governing spatial differences in separation and finding rates: the elasticity of market tightness θ_j to location-specific productivity and the elasticity of the separation threshold level z_j^R to location-specific productivity. Derivations are provided in Appendix B.2.

The elasticity of market tightness to location-specific productivity $\varepsilon_{\theta_j,Z_j}$ takes the following form:

$$\varepsilon_{\theta_j,Z_j} = \underbrace{\Upsilon_j \frac{\mathbb{E}y_j(z')}{\mathbb{E}y_j(z') - c}}_{\substack{\text{Standard} \\ \text{search-and-matching}}} + \underbrace{\Upsilon_j \frac{\mathbb{E}_j y(z')}{\mathbb{E}y_j(z') - c} \Omega_j \varepsilon_{z_j^R,Z_j}}_{\text{Endogenous separations}}, \tag{20}$$

where Υ_j and Ω_j take the following form:

$$\Upsilon_j \equiv \frac{(1-\delta)\beta(1-d)(1-F(z_j^R))\eta p(\theta_j) + (1-(1-\delta)\beta(1-d)(1-F(z_j^R)))}{(1-\delta)\beta(1-d)(1-F(z_j^R))\eta p(\theta_j) + (1-(1-\delta)\beta(1-d)(1-F(z_j^R)))\varepsilon_{q_j,\theta_j}}, \tag{21}$$

$$\Omega_j \equiv \varepsilon_{\mathbb{E}z',z_j^R} + \frac{\mathbb{E}y_j(z') - c}{\mathbb{E}y_j(z')} \left(1 + \frac{\kappa(1-\eta p(\theta_j))}{q(\theta_j)(1-\eta)(\mathbb{E}y_j(z') - c)}\right) \varepsilon_{1-F(z_j^R),z_j^R}. \tag{22}$$

Equation (20) extends the concept of the fundamental surplus introduced in Hagedorn and Manovskii (2008) and Ljungqvist and Sargent (2017) to a spatial equilibrium setting with endogenous separations. In particular, equation (20) shows that the elasticity of market tightness to location-specific productivity $\varepsilon_{\theta_j,Z_j}$ is made of two components.

The first component, scaling also the second, is the product of Υ_j and the inverse of the *fundamental surplus* $(\mathbb{E}y_j(z') - c)/\mathbb{E}y_j(z')$.[13] In the words of Ljungqvist and Sargent (2017), it is the upper bound on the fraction of output that the invisible hand can allocate to capital vacancy creation. Thus, this first component captures how elastic market tightness is to location-specific productivity in the absence of endogenous separations.

The second component, whose strength is also mediated by Υ_j and the inverse of the fundamental surplus $(\mathbb{E}y_j(z') - c)/\mathbb{E}y_j(z')$, captures the role of endogenous separations and is the sum of two terms summarized in Ω_j. The first term captures the effect that z_j^R has on the expected idiosyncratic productivity $\mathbb{E}z'$. This term is positive because a higher separation

[13] Υ_j is a function of the (negative) matching function elasticity, defined as $\varepsilon_{q_j,\theta_j} \equiv \frac{\partial q(\theta_j)}{\partial \theta_j}\frac{\theta_j}{q(\theta_j)}$.

threshold level allows only more productive matches to be sustained, thereby increasing expected idiosyncratic productivity. The second term captures instead the effect that z_j^R has on the survival probability $1-F(z_j^R)$. This term is negative because a higher separation threshold level lowers the survival probability of a match.

Equation (20) reveals under which circumstances the model delivers a small role for the finding rate in driving cross-sectional dispersion in capital unemployment rate, i.e., a small $\varepsilon_{\theta_j,Z_j}$. In particulat, the Ω_j component results from forces acting in opposite directions, which are difficult to characterize without additional assumptions on $F(\cdot)$. However, selecting a uniform distribution for the idiosyncratic productivity process, as commonly done in the literature, enables us to derive a closed-form solution for $\varepsilon_{\mathbb{E}z',z_j^R}$ and $\varepsilon_{1-F(z_j^R),z_j^R}$, which we can demonstrate to be small. Therefore, a small first component is enough to ensure that $\varepsilon_{\theta_j,Z_j}$ is small, and thus, the finding rate does not vary much across locations. For the first component to be small, since equation (21) shows that Υ_j is close to one, it is enough for the fixed operating cost c to be sufficiently small relative to the expected output $\mathbb{E}y_j(z')$, i.e., to have a large fundamental surplus.

The elasticity of the separation threshold level z^R to location-specific productivity $\varepsilon_{z^R,Z}$ takes the following form:

$$\varepsilon_{z_j^R,Z_j} = -\underbrace{1}_{\substack{\text{Direct}\\ \text{effect}}} \underbrace{- \frac{\kappa\theta_j}{(1-\eta)y(z_j^R)}\left(\frac{\varepsilon_{q_j,\theta_j}}{p(\theta_j)} - \eta\right)\varepsilon_{\theta_j,Z_j}}_{\text{Indirect effect}}. \tag{23}$$

The elasticity of the separation threshold level to location-specific productivity $\varepsilon_{z_j^R,Z_j}$ is negative, indicating that higher location-specific productivity lowers the separation threshold level. In standard search-and-matching models with exogenous separations, this elasticity is zero. Equation (23) is composed of two components. The first component captures the direct effect that changes in location-specific productivity have on the separation threshold level. The second component captures the indirect effect that location-specific productivity has on market tightness, captured by the elasticity of market tightness to location-specific productivity $\varepsilon_{\theta_j,Z_j}$, and thus on the value of the firms.

Clearly, if the model succeeds in explaining the large contribution of separations to differences in capital unemployment rates across locations, it is because of a high value for the second term of equation (23). For this to be the case, the term multiplying $\varepsilon_{\theta_j,Z_j}$ must be suffi-

ciently large. This occurs because either $y(z_j^R)$ or η is sufficiently low, or because the effective cost of searching $k\theta_j$ is sufficiently high. In all these cases, the marginal producing firm has a very low value, so a decline in location-specific productivity triggers a strong increase in separations. Additionally, when $\varepsilon_{q_j,\theta_j}$ is sufficiently large, conditional on η, the marginal producing firm also has a very low value due to excessive firm entry, as explained in Section 4.5, making also endogenous separations highly sensitive to location-specific productivity.

Thus, equation (20) and (23) show the channels through which the model can be successful in matching the low contribution of the finding rate and the high contribution of the separation rate to differences in the capital unemployment rate observed in the data. However, whether the model will be quantitatively successful is ultimately a calibration question.

4.4 Spatial Equilibrium

For the spatial equilibrium, since our focus is on the long-run spatial distribution of capital and its unemployment rate, as motivated by the evidence in Section 2, we allow capitalists with unemployed capital to move freely between locations. Thus, following Rosen (1979)-Roback (1982), we assume that the following condition holds in equilibrium:

$$V_j^u = \underline{V} \quad \forall j \in \{1, \ldots, J\}. \tag{24}$$

This equation implies that capitalists owning unemployed capital can move freely across local capital markets, and in equilibrium, the value of searching in different capital markets must be equal.[14] To achieve this, effective cost of managing capital ℓ_j must adjust accordingly. Since $g'(K_j)$ is determined by the size of the location, unobserved amenity values A_j offered by individual locations ultimately ensure that equation (24) is satisfied in equilibrium.

[14]While this assumption is convenient, we emphasize that it is inconsequential for our positive analysis, which seeks to explain, given the distribution of capital across locations, which local forces (finding versus separation rates) shape its unemployment rate. However, this assumption is not inconsequential for the normative implications of the paper, as policies affect both local forces and the incentive to move capital across locations. While using this long-run view as a benchmark, we demonstrate in our quantitative analysis how different assumptions driving the distribution of capital across locations affect the welfare gains of policies.

4.5 Efficiency

This section investigates the model's efficient properties, akin to Kuhn et al. (2021), by characterizing the *constraint* efficient allocation. A social planner, facing the same frictions as the agents, reallocates capitalists with unemployed capital across locations instantaneously. The planner also determines capital vacancies and match destruction in each location, constrained by search frictions. We delineate this allocation in two steps: first, outlining the optimal within-location allocation given an arbitrary distribution of capitalists, and second, deriving the optimal allocation of capitalists across locations.

Given a spatial allocation of capital, the planner chooses (v_j, z_j^R) to maximize the average present discounted value for each location j. The problem can be written recursively as follows:

$$\begin{aligned}\omega(k_j^u, \mathbb{E}y_j) &= \max_{v_j, z_j^R} \; k_j^u V_j^u + (1-k_j^u)\mathbb{E}V_j^e(z) + (1-k_j^u)\mathbb{E}V_j^p(z) + v_j V_j^v \\ &= \max_{v_j, z_j^R} (1-k_j^u)(\mathbb{E}y_j(z) - c) - \kappa v_j + A_j - g_j' + \beta\omega(k_j^{u'}, \mathbb{E}y_j'),\end{aligned} \tag{25}$$

subject to the following low of motion:

$$\begin{aligned}k_j^{u'} = (1-\delta)k_j^u \left(1 - p(\theta_j)(1-d)(1-F(z_j^R))\right) \\ + (1-\delta)(1-k_j^u)\left(1 - (1-d)(1-F(z_j^R)\right) + \delta.\end{aligned} \tag{26}$$

Equation (25) states that the average present discounted value in each location j is the average value in each location. This is subject to the motion law of unemployed capital (26), which mirrors the one specified in the empirical analysis in Section 3.1.

After some algebra, the first-order conditions with respect to v_j and z_j^R, together with the

envelope condition can be characterized by the following three equations:

$$\kappa = (1-\delta)\beta q(\theta_j)(1-d)\mathbb{E}\left[V_j^{p,SP}(z')\right]^+, \tag{27}$$

$$\mathbb{E}V_j^{p,SP}(z) = (1-\varepsilon_{q_j,\theta_j})\left(\mathbb{E}y_j(z) - c\right) - \varepsilon_{q_j,\theta_j}\kappa\theta_j + \frac{\kappa}{q(\theta_j)}, \tag{28}$$

$$0 = (1-\varepsilon_{q_j,\theta_j})\left(y_j(z_j^R) - c\right) - \varepsilon_{q_j,\theta_j}\kappa\theta_j + \frac{\kappa}{q(\theta_j)}; \tag{29}$$

with:

$$\mathbb{E}V_j^{p,SP}(z) \equiv -(1-\varepsilon_{q_j,\theta_j})\frac{\partial\omega(k_j^{u'}, y_j')}{\partial k_j^{u'}}; \tag{30}$$

where $-\partial\omega(k_j^{u'}, y_j')/\partial k_j^{u'}$ is the planner marginal value of an extra employed unit of capital.[15] Thus, equation (30) just says that the social planner allocates to producers a fraction $1-\varepsilon_{q_j,\theta_j}$ of its marginal value of an extra employed unit of capital. The derivations of (27) - (29) can be found in Section B.3 of the Appendix.

The social planner equilibrium conditions characterized by equations (27), (28), and (29), coincide with the decentralized equilibrium charactetized by equations (14), (16), and (17) if and only if $\varepsilon_{q_j,\theta_j} = \eta$, which coincides with the condition in Hosios (1990). To understand the intuition behind this condition, notice that $\varepsilon_{q_j,\theta_j}$ is the elasticity of the expected duration of a capital vacancy with respect to the number of capital vacancies and $1-\varepsilon_{q_j,\theta_j}$ is the expected duration of capital unemployment with respect to unemployed capital. If $\varepsilon_{q_j,\theta_j} > \eta$, then it means that at the margin firms are causing more congestion to other firms than capitalists are causing to other capitalists. Therefore, firms must be "taxed" by the social planner by giving capitalists a higher share in the rental rate bargaining. The two congestion forces offset each other if and only if $\varepsilon_{q_j,\theta_j} = \eta$.

Now we consider the efficient allocation of unemployed capital across locations. The social planner chooses a reallocation of unemployed capital across locations $\{K_j^u\}_{j\in J}$ to maxi-

[15] To understand this relation is enough to notice that $\partial\omega(k_j^{u'}, y_j')/\partial k_j^{e'} = (\partial\omega(k_j^{u'}, y_j')/\partial k_j^{u'})/(\partial k_j^{u'}/\partial k_j^{e'}) = -\partial\omega(k_j^{u'}, y_j')/\partial k_j^{u'}$.

mize total welfare as follows:

$$\begin{aligned}\mathcal{W}_j(K_j^e) &= \max_{\{K_j^u\}_{j\in J}} K_j\omega_j \\ &= \max_{\{K_j^u\}_{j\in J}} K_j^u V_j^{u,SP} + K_j^e \mathbb{E}V_j^{e,SP}(z) + K_j^e \mathbb{E}V_j^{p,SP}(z) + V_j^k V_j^{v,SP} \\ &= \max_{\{K_j^u\}_{j\in J}} K_j^u \tilde{V}_j^{u,SP} + K_j^e \mathbb{E}\tilde{V}_j^{e,SP}(z) - \frac{g(K_j)}{1-(1-\delta)\beta} + K_j^e \mathbb{E}V_j^{p,SP}(z) + V_j^k V_j^{v,SP},\end{aligned} \tag{31}$$

subject to the following constraint:

$$\sum_{j\in J} K_j = K, \tag{32}$$

where $\tilde{V}_j^{u,SP} = \tilde{V}_j^{u,SP} + g'(K_j)/(1-(1-\delta)\beta)$ and $\mathbb{E}\tilde{V}_j^{e,SP}(z) = \mathbb{E}\tilde{V}_j^{e,SP}(z) + g'(K_j)/(1-(1-\delta)\beta)$ are defined as the social planner value, which the outcome of the efficient allocation just define, before deducing the present discounted local cost of managing capital $g'(K_j)$ and K is the total capital across locations.

The social planner's firs-order conditions are as follows:

$$V_j^{u,SP} = \lambda, \tag{33}$$

where λ is the Lagrange multiplier associated with the constrain (32). Thus, the social planner equalizes its value of unemployed capital across locations, mirroring the decentralized equilibrium. As a consequence, once the within-location allocation is fixed, the across-location allocation is also fixed, leading the entire economy to achieve an efficient allocation. This can be achieved with the following place-based subsidy to capitalists with unemployed capital:[16]

$$\tau_j = \frac{\varepsilon_{q_j,\theta_j} - \eta}{1-\eta}\left(\mathbb{E}y_j(z) - c + \kappa\theta_j\right)\Big|_{z_j^R = z_j^{R,SP}, \theta_j = \theta_j^{SP}}. \tag{34}$$

Equation (34) inherits the properties of the social planner within-location allocation described before. When $\varepsilon_{q_j,\theta_j} = \eta$, i.e., when the Hosios (1990) condition holds, the optimal subsidy is zero in all locations. When $\varepsilon_{q_j,\theta_j} < \eta$, the optimal subsidy is negative, meaning it

[16]Note that this place-based subsidy to capitalists with unemployed capital is isomorphic to a place-based tax on firms or capitalists with employed capital.

is optimal to tax capitalists. Conversely, when $\varepsilon_{q_j,\theta_j} > \eta$, the optimal subsidy is positive. In the latter case, the decentralized equilibrium is congested, featuring too many firms relative to the available capitalists in a given location. Thus, to improve upon the decentralized equilibrium, the planner makes capitalists with unemployed capital pickier, which is reflected in higher rental rates. This increases operating costs for firms, thereby easing the congestion externality.

5 Quantification

This section presents the calibration strategy of the model and validates it on several untargeted moments. Then, it assesses the ability of the model to replicate the contribution of different flows to capital unemployment rate differences across locations as established in Section 3.2. Finally, it solves the social planner equilibrium exploring the potential for place-based policies.

5.1 Functional Forms and Calibration

Here, we describe the functional forms used throughout the quantitative analysis and present the calibration strategy.

5.1.1 Functional Forms. In the quantitative analysis we assume the following relation between the cost of managing capital and location size, given by:

$$g'(K_j) = \gamma K_j, \tag{35}$$

where gamma represent the elasticity of the cost of managing capital to location size. We assume the following matching function:

$$M(K_j^u, V_j^k) = m(K_j^u)^\alpha (V_j^k)^{1-\alpha}, \tag{36}$$

where m is the matching efficiency and α is the matching function elasticity, previously defined for a general matching function as $\varepsilon_{q,\theta}$.

Finally, as in Pissarides (2000), we assume that each period a new productivity shock

$z \sim \mathcal{U}[a, b]$ is drawn with probability λ.[17] In line with this interpretation, productivity takes its expected value if no new shock is drawn.[18]

5.1.2 Calibration. The calibration strategy involves two steps: first, fixing parameters estimated outside the model; second, choosing the remaining parameters to match the identifying moment of the data.

Each model period is one year, so β is set at 0.96. We set the depreciation rate to 2 percent, as in the empirical analysis. The matching function elasticity is set to 0.70, which is the lower bound estimate from the micro-data in Ottonello (2021).[19] This must be interpreted as a conservative choice, as a high value of this elasticity will increase the role of the separation rate in explaining spatial capital unemployment gaps, as explained in Section 4.3. We set the exogenous separation rate to 0.01, which is close to the minimum separation rate measured in our data and to the level in Ottonello (2021). The probability of match-specific shocks is set to 0.10, implying a persistence of 0.90, which is close to Foster et al. (2008) and well within the range reported by the literature, ranging from 0.97 in Lee and Mukoyama (2015) to 0.5 in Ábrahám et al. (2006) and Castro et al. (2015). Following Kuhn et al. (2021), we set the upper bound of the match-specific shock b to 2 and the lower bound a to 1 so that the unconditional average is 1. Finally, we normalize the exogenous productivity of the median capital unemployment rate location of 1.

Thus, seven parameters remain to be calibrated: the matching efficiency m; the capital vacancy posting cost κ; the fixed operating cost c; the capitalists bargaining power η; the managing capital cost parameter γ; and the maximum and minimum location-specific exogenous productivities.

We inform model parameters Z_{min}, η, and Z_{max} using the maximum, median, and minimum observed capital unemployment rates across locations, which are 16 percent, 9 percent, and 4 percent, respectively. The maximum capital unemployment rate informs the minimum productivity since there is a one-to-one inverse mapping between the two, and the same applies for $Z_{\max}$ and the minimum capital unemployment rate. The bargaining power of capitalists, η, is an important parameter in the model governing the efficiency of the equilibrium

[17] We chose this functional form for the distribution of z to align with the literature. However, Kuhn et al. (2021) show that this assumption is relatively inconsequential for this class of models.

[18] This formulation allows to reproduce a leptokurtic idiosyncratic shock distribution, which is empirically supported by Bachmann and Bayer (2014).

[19] This value is close to those in macro-labor, such as empirical estimates reported by Petrongolo and Pissarides (2001) and the parameterization in Shimer (2005).

Table 2: Parameters

Parameter	Description	Value
Fixed		
β	Discount factor	0.96
δ	Depreciation rate	0.02
α	Matching function elasticity	0.70
d	Exogenous separation rate	0.01
λ	Probability of match-specific shocks	0.10
b	Match-specific shock upper bound	2
a	Match-specific shock lower bound	0
Z_{median}	Median productivity	1
Fitted		
m	Matching efficiency	0.123
κ	Capital vacancy posting cost	0.002
c	Fixed operating cost	0.876
η	Capitalists bargaining power	0.375
γ	Cost of managing capital elasticity	5.398
Z_{max}	Maximum productivity	1.154
Z_{min}	Minimum productivity	0.919

and is inversely related to capital vacancy creation in all locations, thus affecting the median unemployment rate. The calibration of m is informed by the median location finding rate of 40 percent. The capital vacancy posting cost is informed by a separation rate of 2 percent as it pins down the expected value of producing for a firm, thus affecting the level of matches that can be sustained in equilibrium and, as a consequence, the separation threshold level. Another important parameter is the fixed operating cost c, which determines the size of the fundamental surplus and thus the relative importance of the finding versus separation rate in driving capital unemployment rate gaps. Since this parameter affects the total costs of the firm, we inform it by targeting an average capital cost share, measured as the ratio of capital cost to total costs, which is 11 percent according to De Loecker et al. (2020). Finally, as systematic studies analyzing the cost of managing capital in the UK are not readily available, we estimate a plausible range of numbers based on the fees charged by a leading real estate service company, Savills. Savills reports a fee range between 15 and 30 percent of the total rental cost of real estate.[20] Therefore, we calibrate the parameter γ to reflect a cost of managing capital equivalent to 25 percent of the rental rate, which falls within the range mentioned.

The parameters are jointly estimated using a search algorithm in the parameter space

[20] Source: Savills.co.uk

Table 3: Moments

Moment	Data	Model
Maximum capital unemployment rate	0.16	0.16
Median capital unemployment rate	0.09	0.09
Minimum capital unemployment rate	0.04	0.04
Separation rate	0.03	0.03
Finding Rate	0.40	0.40
Capital costs share	0.11	0.10
Cost of managing capital to rental rate	0.25	0.25

Note. The table presents parameter values and target moments from both the model and the data.

that minimizes the distance between the empirical and simulated moments. The parameters implied by the calibration strategy of the model are presented in Table 2. Table 3 shows the fit of the model on several identifying moments. Even though the model is nonlinear, it fits the target moments satisfactorily. Unfortunately, as local capital markets have been relatively understudies due to the lack of available data, there is no widely accepted empirical estimate for most of the parameters. However, we note that a capitalist bargaining power η of 0.375 and a fixed cost c of 0.876 generate a profit share of 0.035 in the median capital unemployment rate location, well within the 0-0.10 range found by Barkai (2020) and De Loecker et al. (2020) for the period from 1980 to the present days. Further validations on η are postponed to Section 5.3, where we delve into the normative implications of the model. While η plays a minor role in the model's positive implications, it is crucial for its normative implications. Next, we proceed to explore and validate the model's positive performance on several untargeted moments.

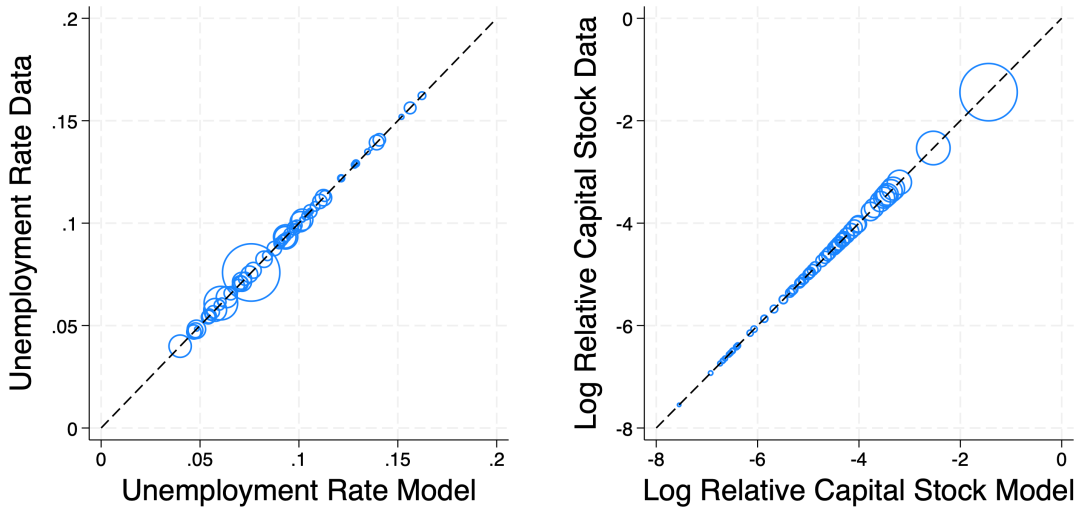
5.2 Quantitative Performance of the Model

This section validates the quantitative performance of the model on many untargeted moments and assesses its ability to match the quantitative importance of the separation rate in driving spatial capital unemployment gaps, as documented in Section 3.2.

5.2.1 Model Validation. Here we asses the quantitative performance of the model on many untargeted moments.

Additional calibration. Before assessing the model performance on the untargeted moments, we need to augment the calibration form Section 5.1 to pin down local productivities

Figure 6: Capital Unemployment Rate and Capital Stock



(a) Capital Unemployment Rate **(b) Capital Stock**

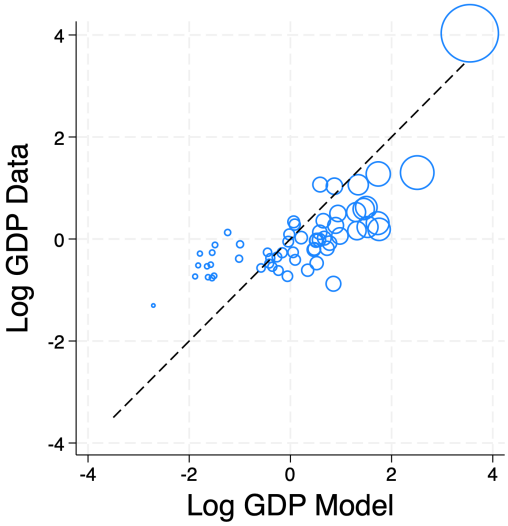
Note: Figure 6 presents a comparison of capital unemployment rates and total capital between the model and UK data. In Figure 6a, blue circles represent unemployment rates from the model plotted against those from the data, with a dashed black 45-degree line for reference. In Figure 6b, blue circles represent the total capital from the model plotted against that from the data, also with a dashed black 45-degree line for reference. The size of the circles corresponds to the size of the location.

Z_j and the local amenities A_j in our J locations in the data.[21] For productivities Z_j, we follow the approach outlined in Section 5.1 and inform it by the local capital unemployment rates. We inform amenities A_j with the distribution of capital across locations, where the location capital is normalized so that the total capital in the economy equals one in the model. Figure 6 compares the model-implied capital unemployment rate (Figure 6a) and total capital (Figure 6b) with the corresponding empirical values. Both figures show a close match between the capital unemployment rate and the total capital in the model and the data, as indicated by their alignment to the 45-degree line, which highlights that the model is successful in matching those additional moments used in this augmented calibration.

Relative GDP by location. To validate the model, we begin by noting that local productivities, along with total local capital, determine the GDP of our locations up to the equilibrium location-specific separation thresholds level. Therefore, it is natural to employ this untargeted moment and compare it with the data to evaluate the performance of our calibration strategy. Figure 7 plots the local GDP in the model against the one in the data. The model matches GDP

[21] For precision, we need to calibrate only $J - 3$ productivity levels, as the maximum, median, and minimum have already been calibrated in the main calibration strategy in Section 5.1.

Figure 7: Output: Model vs. Data



Note: Figure 7 scatterplots log GDP across cities in the UK from the model and data, with cross-sectional means removed. GDP in the model is calculated as capital productivity times capital stock. The dotted line represents the 45-degree line.

well in the data, as shown visually and by a correlation of 0.74 between the GDP of the model and that in the data.

Rental rates. In Section 5.3.1, we compare the relationship between the capital unemployment rate and the rental rate of capital. This relationship reveals the sensitivity of rental rates to changes in local capital market conditions. Overall, we find that the model's qualitative and quantitative predictions align well with the data.

Amenities. Unobserved local amenities allow the model to match the distribution of capital across locations. A natural check of the nonparametric amenity estimates A_j is to correlate them with local characteristics that should affect the value of operating capital in a particular location. We correlate the estimated amenities with an amenity score provided by PMA,[22] as well as with ONS data on the location's average distance from a train station, airport, and hospital. Online Appendix Table C.4 shows that a higher amenity score is positively associated with higher amenities, while larger distances from a train station, airport, and hospital are associated with lower amenities. These results support the view that estimated amenities capture salient features of the attractiveness of operating capital in a particular location.

Having established the ability of the estimated model to speak to a number of targeted

[22]PMA's amenity scores are based on the presence of key anchor stores, national and regional fashion, non-fashion, and food & beverage multiples within each retail location. The scores reflect both the size and quality of key anchor stores, variety stores, and fashion multiples. A high score indicates stronger retail provision.

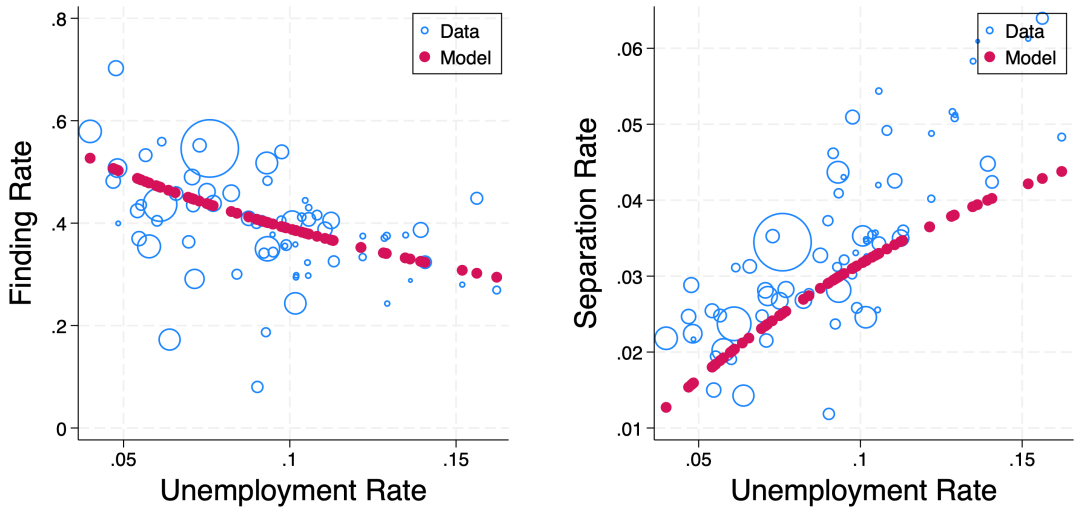
and non-targeted moments, such as relative GDP distribution across locations, rental rates, and amenities, we now turn to the main structural results.

5.2.2 Spatial Capital Unemployment Gaps Decomposition. Here, we now assess its ability to explain quantitatively the salient feature of local capital markets documented in Section 3.2.

Figure 8 displays the finding (Figure 8a) and separation rates (Figure 8b) across UK locations in the data (blue) and the model (red). The left panel illustrates a decrease in finding rates as we move from locations with low capital unemployment rates to those with high capital unemployment rates. The right panel shows an increase in separation rates with the capital unemployment rate. It is important to note that in our calibration we target only the finding and separation rates at the median capital unemployment rate location, targeting neither the role of finding rate and separation rates in determining capital unemployment rate differences across locations nor differences in capital vacancy posting or market tightness. Thus, despite not being targeted, the model aligns closely with the data, both qualitatively and quantitatively. When comparing spatial variations, we notice that finding rates exhibit considerably less variability than separation rates. Specifically, the separation rate in the capital market with the highest capital unemployment rate is more than three times as high as in the capital market with the lowest capital unemployment rate. In contrast, the finding rate is only 44 percent lower in the location with the highest capital unemployment rate compared to the location with the lowest capital unemployment rate.

A close alignment with the observed patterns of finding and separation rates across space suggests that the model effectively replicates the relative significance of these two flow rates in driving spatial capital unemployment gaps. This can be seen in Figure 9, which presents the decomposition of the local capital unemployment rate differences between its different capital-flows, i.e., finding rate (Figure 9a) and separation rate (Figure 9b), from the model (red) and the data (blue) from Figure 4. The formal decomposition reveals a tight match between the model and data. In the model, separation rates account for 68 percent of the cross-sectional variation in capital unemployment rates, compared to 68 percent in the data, while finding rates contribute to 32 percent of the cross-sectional variation in capital unemployment rates in the model, close to the 30 percent observed in the data. These calculations have been done as in Section 3.2 assuming δ close to zero. Appendix C presents the calculations for the

Figure 8: Finding and Separation Rate across Local Capital Markets: Model vs. Data



(a) Finding Rate **(b) Separation Rate**

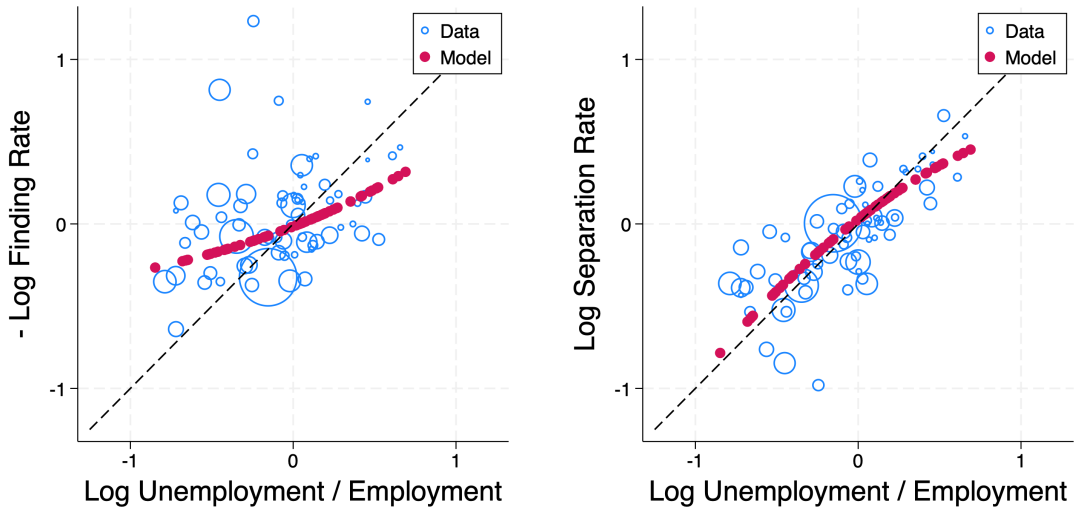
Note: Figure 8 shows finding rates and separation rates from the model (red) and the data (blue) across UK locations. Figure 8a shows finding rates. Figure 8b shows separation rates. The size of the circles is proportional to the size of the location.

general case, highlighting the contribution of the extensive margin and showing that the same takeaways hold.

To understand the success of the model in explaining the small contribution of the finding rate and the large contribution of the separation rate to local capital unemployment rate differences, it is helpful to refer to Section 4.3. First, the model generates a low elasticity of market tightness to productivity and thus of finding rate. This is because the calibration implies a sufficiently large fundamental surplus, as required by equation (20), which is due to the fixed cost c being sufficiently smaller than $\mathbb{E}y(z')$. Second, the model yields a high elasticity of the separation threshold level to productivity and hence of the separation rate. As shown in equation (23), this occurs when the term multiplying the elasticity of market tightness to productivity is sufficiently high, i.e., when the marginal producing firm has a low value, as recovered by our calibration.

Thus, having established the ability of the model to speak to several targeted and untargeted moments and demonstrated its consistency with the data in explaining local capital unemployment gaps, we now shift our focus to studying the efficient allocation in this economy and exploring the potential for place-based policies.

Figure 9: Decomposition of Spatial capital unemployment Gaps: Model vs. Data



(a) Finding Rate **(b) Separation Rate**

Note: Figure 9 illustrates the contribution of minus the log of the finding rate and the log of the separation rate to local capital unemployment rate differences in the model (blue) and data (red), across UK locations. In Figure 9a, minus the log of the finding rate is plotted against the log of the unemployment-employment capital ratio, along with the dashed black 45-degree line. Figure 9b displays the log of the separation rate against the log of the unemployment-employment capital ratio, also with the dashed black 45-degree line. The size of the circles is proportional to the size of the location.

5.3 Social Planner Solution and Place-Based Policies

This section explores the normative implications of the theory. First, it validates the calibrated bargaining power of the capitalists, then explores quantitatively the implications of place-based policies, and finally puts these policy implications into perspective by discussing the model's limitations.

5.3.1 Capitalists' Bargaining Power Validation. The calibrated model reveals that capitalists' bargaining power is lower than the matching function elasticity, implying, as explained in Section 4.5, that the decentralized equilibrium is inefficient with too many firms relative to capitalists. Before quantifying the welfare losses arising from this inefficiency, this section further validates the calibrated parameters of the model, demonstrating that the capitalists' bargaining power implied by the calibration is consistent with the data.

To do so, we exploit Equation (15) to derive a unit-free relation between the rental rate and the capital unemployment rate. It can be shown that the rental rate elasticity of the capital

unemployment rate in a given location is as follows:

$$\varepsilon_{r_j,k_j^u} = -\eta \frac{\kappa \theta_j}{\mathbb{E} r_j(z)}. \tag{37}$$

Equation (37) shows that an increase in the capital unemployment rate leads to an unambiguous decline in the rental rate, and the strength of this decline is mediated by η, the bargaining power of capitalists. Therefore, we can measure this elasticity in the data and compare it to the model to validate our calibration of the bargaining power of capitalists.

Table 4: Rental Rate Elasticity of Capital Unemployment Rate: Model vs. Data

Dependent Variable	**Rental Rate**		
	Data (OLS)	Data (TSLS)	Model
	(1)	(2)	(3)
Capital unemployment rate	-0.12**	-0.49***	-0.50
	(0.05)	(0.13)	
Fixed Effects			
City	✓	✓	
Time	✓	✓	
Controlls			
City-specific Time Trend	✓	✓	
Observations	743	443	

Note. Both the rental rate and the capital unemployment rate are in logs. City-specific time trends are quadratic. Column (1) performs a simple OLS, while column (2) performs a TSLS where the capital unemployment rate is instrumented with labor productivity. Column (3) reports the theoretical elasticity in the model. $^{+}$,*, **, and *** denote 15, 10, 5, and 1% statistical significance respectively.

Table 4 performs this comparison. Columns (1) and (2) regress the log of the rental rate against the log of the capital unemployment rate, where the former is measured as the present value of future prices.[23] Column (1) presents a simple OLS regression. However, our empirical setting is prone to both measurement error and omitted-variable bias. While the former clearly biases our estimates downward, the impact of the latter is unclear. To address these concerns, in column (2) we use a TSLS estimator with log labor productivity as an instrument for log capital unemployment rate. Column (3) reports the theoretical elasticity (37) from the model.

We find a statistically significant negative rental rate elasticity of the capital unemploy-

[23]Formally, we measure the rental rate per square meter in each location as the present value of local prices per square meter given by $r_j = \frac{p_j}{1-(1-\delta)\beta}$.

ment rate in the data, as predicted by the model. Moreover, once correcting for measurement error and omitted-variable bias, we find magnitudes that are closely aligned between the model and the data. Specifically, we find an elasticity of -0.49 in the data and -0.50 in the model. Overall, this supports our calibration, which indicates that capitalists' bargaining power is substantially lower than the matching function elasticity. Having provided additional evidence suggesting the likely inefficiency of the decentralized equilibrium, we move in the next section to quantify the gains from implementing optimal place-based policies.

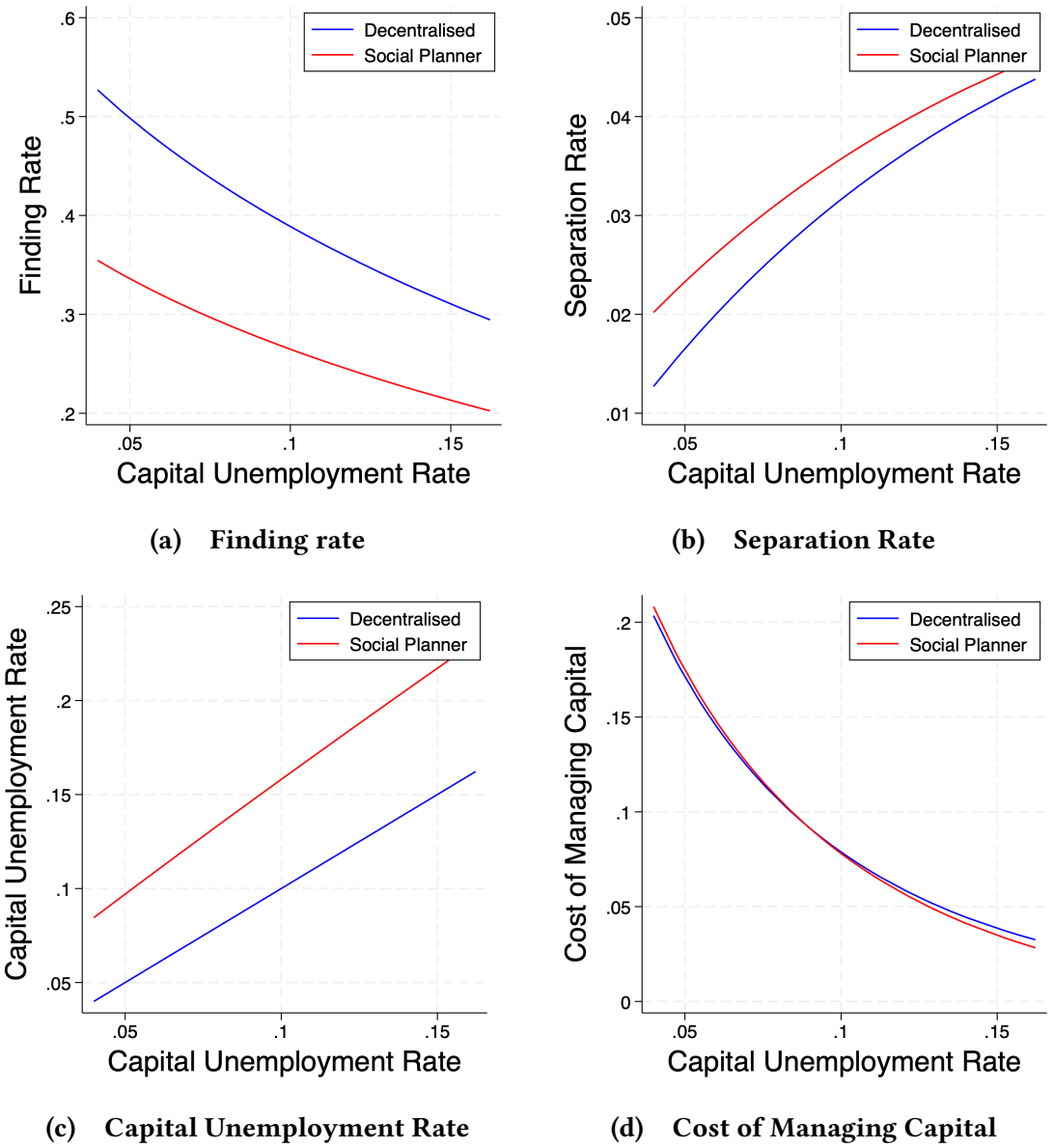
5.3.2 Place-Based Policy Quantification. This section explores quantitatively the implications of place-based policies. Figure 10 shows the finding rate, the separation rate, the capital unemployment rate, and the effective cost of managing capital for the decentralized equilibrium (blue) and social planner's equilibrium (red) as a function of the capital unemployment rate in the decentralized equilibrium.

As we recover α being larger than η, as explained in Section 4.5, firms cause more congestion to other firms than capitalists cause to other capitalists. Thus, by subsidizing capitalists with unemployed capital, the social planner effectively gives them a higher share in the rental rate bargaining. Furthermore, the social planner allocates more subsidies to highly congested locations, which are also the most productive. Figures 10a and 10b show that the social planner commands a lower finding rate and a higher separation rate. This results from giving capitalists a higher share in rental rate bargaining, which discourages firm entry and vacancy creation, leading to lower market tightness and finding rates. It also reduces the value of firm operations, raising the threshold productivity level at which firms can operate, thus increasing the separation rate.

Because the finding rate captures outflows from the unemployed capital stock and the separation rate captures inflows in the unemployed capital stock, a lower finding rate, and higher separation rate translate into a higher capital unemployment rate, as shown in Figure 10c. Thus, the social planner aims to tighten the market on the capitalists' side and loosen it on the firm side, leaving more capital available for use by the firms, consequently increasing the capital unemployment rate.

Finally, by giving capitalists a higher share in the rental rate bargaining, the value of having unemployed capital increases, but more than proportionally for low capital unemployment rate locations. Thus, as the social planner aims to equalize this value across locations, it

Figure 10: Social Planner and Decentralised Equilibrium



(a) Finding rate **(b) Separation Rate**

(c) Capital Unemployment Rate **(d) Cost of Managing Capital**

Note: In Figure 10, we show several outcomes for the decentralized equilibrium (blue) and social planner's equilibrium (red) as a function of the capital unemployment rate in the decentralized equilibrium. Figure 10a shows the finding rate. Figure 10b shows the separation rate. Figure 10c shows the capital unemployment rate. Figure 10d shows the capital managing cost.

moves capitalists from the high capital unemployment rate locations to the low capital unemployment rate ones, tilting the effective cost of managing capital in favor of the high capital unemployment rate locations. Figure 10d shows this tilting, resulting in a lower effective cost of living for high capital unemployment rate locations and a higher one for low capital unemployment rate locations.

Having explained the mechanism behind the social planner allocation, we move now to

analyze the welfare implications of this allocation compared to the decentralized one. Since we aim to compare between different long-run equilibria, we focus on steady-state comparisons. Steady-state per capita welfare can be expressed as follows:

$$\begin{aligned}\omega_j^{TOT} &= \frac{1}{1-\beta}\left((1-k_j^u)(\mathbb{E}y_j(z)-c)-\kappa v_j + A_j - g_j'\right), \\ &= \omega_j^{S\&M} + \omega_j^{SE};\end{aligned} \tag{38}$$

where:

$$\omega_j^{S\&M} = \frac{1}{1-\beta}\left((1-k_j^u)(\mathbb{E}y_j(z)-c)-\kappa v_j\right), \tag{39}$$

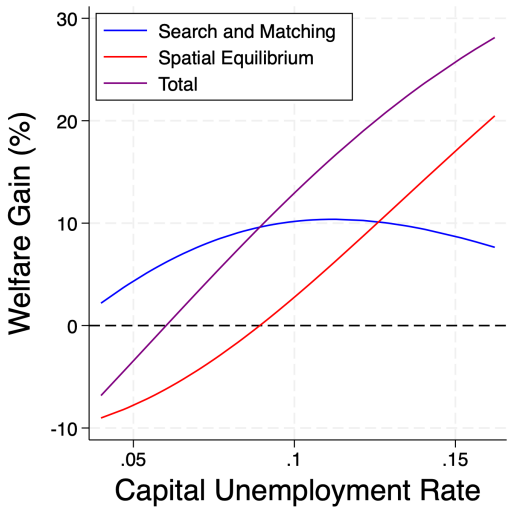
$$\omega_j^{SE} = \frac{1}{1-\beta}\left(A_j - g_j'\right). \tag{40}$$

Thus, welfare can be decomposed into a first component due to the search-and-matching structure embedded $\omega_j^{S\&M}$ in the model and a second component due to the spatial equilibrium ω_j^{SE}. This decomposition is helpful because it allows us to gauge the extent to which the assumption of perfect capital mobility motivated by our long-run view, discussed in Section 4.4, influences our normative conclusions.

This is the case because, while $\omega_j^{S\&M}$ captures only within-location forces (equations (27)-(29)), taking the distribution of capital as given, ω_j^{SE} captures the role played by the free reallocation of capital, influencing the marginal cost of managing capital in a given location g_j'. Thus, while the former informs us about the welfare gains conditional on the distribution of capital (i.e., when capital cannot relocate), the sum of the former and the latter component tells us the welfare gain in the opposite scenario, where capital is freely mobile. We will exploit this difference in Section 5.3.3 when we discuss some of the limitations of our framework and their effects on our normative conclusions.

Figure 11 shows the percentage change in welfare and all its components across the different locations, sorted by their capital unemployment rate level. First, we notice that the search-and-matching component of welfare exhibits an increase across all locations. This is unsurprising since the social planner imposes the Hosios (1990) condition, thus improving the decentralized search-and-matching allocation. Second, the spatial equilibrium component of welfare decreases for low capital unemployment rate locations and increases for high ones, as

Figure 11: Welfare Gains from Social Planner Allocation



Note: Figure 11 shows the percentage change in welfare and all its components across the different locations, sorted by their capital unemployment rate level. The search-and-matching component of welfare is in blue. The spatial equilibrium component is in red. Total welfare is in purple.

the outcome of the tilting in the effective cost of managing capital in favor of the latter ones as depicted in Figure 10d.

All these factors taken together imply that total welfare would increase in high capital unemployment rate locations, where the gains from imposing the Hosios (1990) condition are not eroded by the increase in the effective cost of managing capital due to the reallocation of capitalists, but decreases for low capital unemployment rate locations. Our quantification shows that such welfare changes can be large, going from almost 30 percent higher welfare in the highest capital unemployment rate location to almost 10 percent lower welfare in the lower capital unemployment rate location. Moreover, we find that the average welfare in the economy would increase by approximately 4 percent.

5.3.3 Model Discussion and Results Interpretation. Our normative analysis is mostly exploratory and subject to potential caveats.

First, throughout the paper, we assumed that capital is freely mobile across locations. While this does not affect our positive analysis in Section 5.2, which hinges only on within-location forces, it can affect our normative conclusions. Specifically, in the presence of fixed capital—i.e., when capital cannot reallocate—our welfare analysis, captured by the term $\omega_j^{S\&M}$, suggests an average welfare increase of 8.6 percent, substantially higher than the 4 percent increase observed under perfect capital mobility. Additionally, with fixed capital, every loca-

tion gains from place-based policies, whereas with free capital mobility, only the more disadvantaged locations gain. This disparity arises because capital mobility increases the cost of managing capital in the most productive locations, thereby diminishing some of their gains. Overall, these results suggest that positive welfare gains are robust to different assumptions regarding capital mobility. Likely, in the presence of imperfect capital mobility, welfare gains will fall between these two scenarios.

Second, the model abstracts from forces such as agglomeration externalities, additional congestion externalities, and employment considerations, which have been shown to be important determinants for place-based policies in other contexts. Specifically, agglomeration externalities would likely strengthen our mechanism by increasing the incentive to move capitalists to the most productive locations, while additional congestion externalities would act in the opposite direction. Furthermore, although employment considerations may not affect the qualitative predictions of our model, they are likely important in determining the quantitative implications of any analysis on place-based policies. For example, Manning and Petrongolo (2017) and Kuhn et al. (2021) show that if local labor markets are highly localized or efficient, the effect of place-based policies may be small or undesirable. On the other hand, Kline and Moretti (2013) and Bilal (2023) demonstrate that in the presence of hiring costs or significant congestion externalities from firm sorting across locations, place-based policies can have strong leveling-up effects.[24] Considering all these forces together with the mechanism outlined in this paper is beyond our scope. While we recognize that our normative analysis is mostly exploratory, we believe that the mechanism we present introduces an important new element to the analysis of the desirability of place-based policies, with potentially substantial quantitative impact.

6 Conclusion

This paper introduces a novel dataset to provide an initial insight into the distribution of capital utilization, defined by its unemployment rate. We find significant and persistent differences in capital unemployment rates across locations. More prosperous locations are associated with lower capital unemployment rates, and capital investment is small and does not

[24] We emphasize that our place-based policy of subsidizing unemployed capitalists can be equally framed as taxing firms, particularly in more productive locations. This approach is qualitatively aligned with the findings in Bilal (2023), which suggest that firms should be incentivized to move towards less productive locations.

seem to move to close these differences. We propose a spatial decomposition to highlight the role of capital flows into and out of unemployment in understanding the drivers of these persistent capital unemployment rate differences. Our decomposition underscores the major role of inflows into unemployment, which we label separation rates.

We then propose a spatial search-and-matching model of local capital markets with endogenous separations to analyze the economic forces driving the major role of separations behind persistent capital unemployment rate differences across locations. The model explains these phenomena quantitatively well. Finally, we use the model to assess the efficiency of these persistent capital unemployment rate differences across locations. The calibrated model finds that the decentralized equilibrium is inefficient and that there are ample margins for welfare improvements, providing a rationale for place-based policies.

References

Ábrahám, Á., K. White, et al. (2006). The dynamics of plant-level productivity in us manufacturing. *Center for Economic Studies Working Paper 6*, 20.

Allen, T. and D. Donaldson (2022). Persistence and path dependence: A primer. *Regional Science and Urban Economics 94*, 103724.

Bachmann, R. and C. Bayer (2014). Investment dispersion and the business cycle. *American Economic Review 104*(4), 1392–1416.

Barkai, S. (2020). Declining labor and capital shares. *The Journal of Finance 75*(5), 2421–2463.

Bilal, A. (2023). The geography of unemployment. *The Quarterly Journal of Economics 138*(3), 1507–1576.

Castro, R., G. L. Clementi, and Y. Lee (2015). Cross sectoral variation in the volatility of plant level idiosyncratic shocks. *The Journal of Industrial Economics 63*(1), 1–29.

De Loecker, J., J. Eeckhout, and G. Unger (2020). The rise of market power and the macroeconomic implications. *The Quarterly Journal of Economics 135*(2), 561–644.

Den Haan, W. J., G. Ramey, and J. Watson (2000). Job destruction and propagation of shocks. *American economic review 90*(3), 482–498.

Diamond, P. A. (1982). Aggregate demand management in search equilibrium. *Journal of political Economy 90*(5), 881–894.

Foster, L., J. Haltiwanger, and C. Syverson (2008). Reallocation, firm turnover, and efficiency:

Selection on productivity or profitability? *American Economic Review 98*(1), 394–425.

Fujita, S. and G. Ramey (2009). The cyclicality of separation and job finding rates. *International Economic Review 50*(2), 415–430.

Gavazza, A. (2011). The role of trading frictions in real asset markets. *American Economic Review 101*(4), 1106–1143.

Genesove, D. and L. Han (2012). Search and matching in the housing market. *Journal of urban economics 72*(1), 31–45.

Hagedorn, M. and I. Manovskii (2008). The cyclical behavior of equilibrium unemployment and vacancies revisited. *American Economic Review 98*(4), 1692–1706.

Han, L. and W. C. Strange (2015). The microstructure of housing markets: Search, bargaining, and brokerage. *Handbook of regional and urban economics 5*, 813–886.

Hosios, A. J. (1990). On the efficiency of matching and related models of search and unemployment. *The Review of Economic Studies 57*(2), 279–298.

Jung, P., P. Korfmann, and E. Preugschat (2023). Optimal regional labor market policies. *European Economic Review 152*, 104318.

Kitson, M. and J. Michie (2014). *The deindustrial revolution: the rise and fall of UK manufacturing, 1870-2010*. Centre for Business Research, University of Cambridge Cambridge, UK.

Kleinman, B., E. Liu, and S. J. Redding (2023). Dynamic spatial general equilibrium. *Econometrica 91*(2), 385–424.

Kline, P. and E. Moretti (2013). Place based policies with unemployment. *American Economic Review 103*(3), 238–243.

Kuhn, M., I. Manovskii, and X. Qiu (2021). The geography of job creation and job destruction. Technical report, National Bureau of Economic Research.

Lee, Y. and T. Mukoyama (2015). Productivity and employment dynamics of us manufacturing plants. *Economics Letters 136*, 190–193.

Ljungqvist, L. and T. J. Sargent (2017). The fundamental surplus. *American Economic Review 107*(9), 2630–2665.

Manning, A. and B. Petrongolo (2017). How local are labor markets? evidence from a spatial job search model. *American Economic Review 107*(10), 2877–2907.

Marinescu, I. and R. Rathelot (2018). Mismatch unemployment and the geography of job

search. *American Economic Journal: Macroeconomics 10*(3), 42–70.

Mortensen, D. T. (1982). The matching process as a noncooperative bargaining game. In *The economics of information and uncertainty*, pp. 233–258. University of Chicago Press.

Ngai, L. R. and S. Tenreyro (2014). Hot and cold seasons in the housing market. *American Economic Review 104*(12), 3991–4026.

Ottonello, P. (2021). Capital unemployment. *Review of Economic Studies (Conditionally Accepted)*.

Petrongolo, B. and C. A. Pissarides (2001). Looking into the black box: A survey of the matching function. *Journal of Economic literature 39*(2), 390–431.

Pissarides, C. A. (1985). Short-run equilibrium dynamics of unemployment, vacancies, and real wages. *The American Economic Review 75*(4), 676–690.

Pissarides, C. A. (2000). *Equilibrium unemployment theory*. MIT press.

Ramey, V. and M. Shapiro (1998). Capital churning. *Manuscript. Downloaded from http://econweb. ucsd. edu/~ vramey/research/capchrn2. pdf*.

Ramey, V. A. and M. D. Shapiro (2001). Displaced capital: A study of aerospace plant closings. *Journal of political Economy 109*(5), 958–992.

Rice, P. G. and A. J. Venables (2021). The persistent consequences of adverse shocks: how the 1970s shaped uk regional inequality. *Oxford Review of Economic Policy 37*(1), 132–151.

Roback, J. (1982). Wages, rents, and the quality of life. *Journal of political Economy 90*(6), 1257–1278.

Rosen, S. (1979). Wage-based indexes of urban quality of life. *Current issues in urban economics*, 74–104.

Şahin, A., J. Song, G. Topa, and G. L. Violante (2014). Mismatch unemployment. *American Economic Review 104*(11), 3529–3564.

Schmutz, B. and M. Sidibé (2019). Frictional labour mobility. *The Review of Economic Studies 86*(4), 1779–1826.

Shimer, R. (2005). The cyclical behavior of equilibrium unemployment and vacancies. *American economic review 95*(1), 25–49.

Shimer, R. (2012). Reassessing the ins and outs of unemployment. *Review of Economic Dynamics 15*(2), 127–148.

Employed and Unemployed Capital in Space

Andrea Chiavari and Charles Cheng Zhang

Online Appendix

A Data Appendix

A.1 Data Cleaning and Summary Statistics

We leverage a comprehensive dataset sourced from PMA encompassing office, industrial, and logistic buildings at the city level from 1981 to 2022.[25] To get a comprehensive picture of spatial capital allocations, we combine all commercial real estate within each city.

Table A.1: Summary Statistics (1990-2022)

Variables	**Mean**	**S.D.**	**P25**	**P50**	**P75**	**N**
			United Kingdom			
Unemployment Rate	0.10	0.04	0.06	0.09	0.12	987
Employment Rate	0.90	0.04	0.87	0.91	0.93	987
Investment Rate	0.11	1.26	0.01	0.02	0.03	986
Finding Rate	0.40	0.21	0.24	0.38	0.53	987
Separation Rate	0.04	0.02	0.02	0.03	0.05	987
Stock	2645	5343	571	1402	2797	987
			European Union			
Unemployment Rate	0.09	0.04	0.06	0.09	0.12	358
Employment Rate	0.91	0.04	0.88	0.91	0.94	358
Investment Rate	0.03	0.22	0.03	0.04	0.05	357
Finding Rate	0.52	0.20	0.35	0.50	0.67	358
Separation Rate	0.03	0.02	0.02	0.03	0.04	358
Stock	9489	8901	4622	7468	10568	358

Note: Table A.1 presents summary statistics of the capital unemployment rate, employment capital rate, investment rate, finding rate, separation rate, and total capital stock at the city level between 1990 and 2022 for the United Kingdom and Europe. The unit for stock is thousands of square meters.

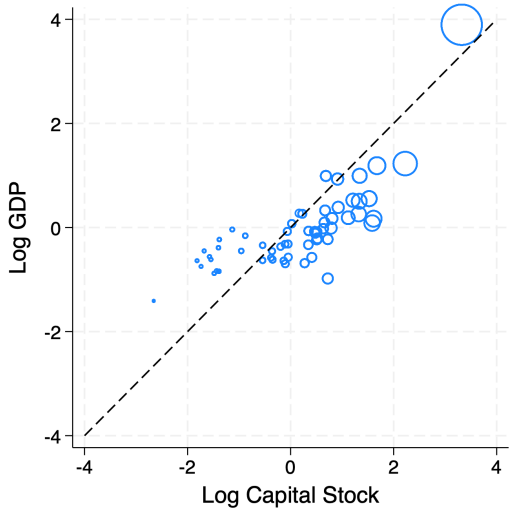
Additionally, we define the investment rate as investment over the capital stock and calculate investment based on equation (5). We derive the finding rate and separation rate according to equations (6) and (7). To ensure data quality, instances where the finding rate and separation rate exceed 0.99 or fall below 0.01 are treated as anomalies and are consequently excluded from our analysis. Moreover, we restrict our analysis to data from 1990 onwards, as this marks a point when the data collection process of the company appears to have reached a sufficiently advanced stage. Table A.1 presents the summary statistics after cleaning the data.

[25] For London and Paris, PMA data are reported at the submarket level, which we aggregate to the city (market) level to ensure consistency across cities.

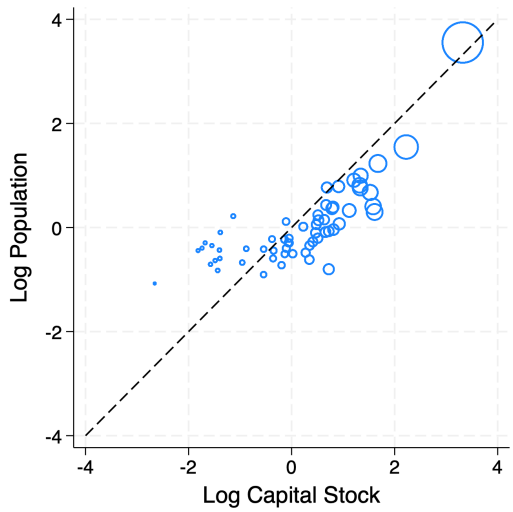
A.2 Data Validation

This section conducts additional validations of the capital stock measures reported by PMA, comparing this data with Ottonello (2021) and across space and over time with well-established measures from UK national accounting provided by the Office of National Statistics (ONS).

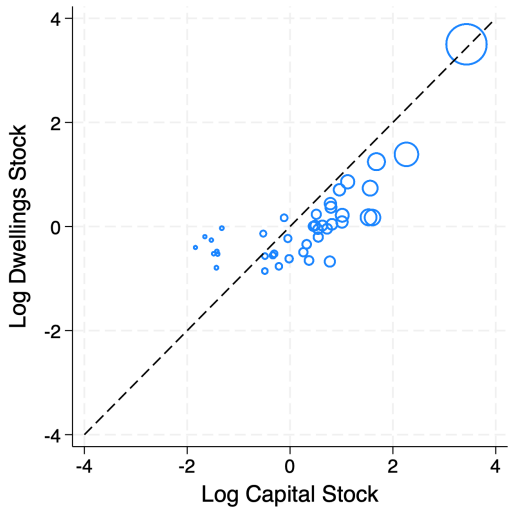
Figure A.1: Spatial Correlations Between PMA Capital Stock and GDP, Population, and Dwellings in the UK



(a) GDP



(b) Population



(c) Dwellings

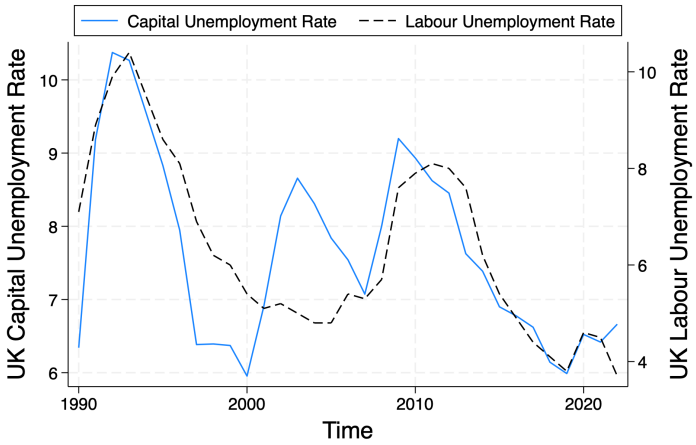
Note: Figure 1 presents the spatial correlation between the capital stock from the PMA dataset and key economic indicators of location size, namely GDP (Figure A.1a), population (Figure A.1b), and dwellings (Figure A.1c) in the UK. All observations are in logs and time-averaged. Cross-sectional averages have been removed. The relative size of each location within the UK is represented by the size of the circles in the figures.

First, we notice that Table A.1 reports summary statistics in line with those reported by Ottonello (2021). In particular, we find that our capital unemployment rate is also 10 percent and that our standard deviation is 4 percent, close to the 2.4 percent found in their study.

Second, we compare our capital stock measure with other measures of location size such as GDP, population, and dwelling stocks. The ONS defines a dwelling as a unit of accommodation that may comprise one or more household spaces (a household space is the accommodation used or available for use by an individual household).[26] Figure A.1 presents the scatterplots of local GDP, population, and dwellings against local capital stock from PMA in the cross-section of UK cities. A visual analysis confirms the expectation that areas with higher GDP, population, and dwellings tend to exhibit higher levels of capital stock.

Finally, we follow Ottonello (2021) and compare the behavior over time of the capital unemployment rate with the normal unemployment labor rate. Figure A.2 illustrates this comparison over time. Overall, we observe that the dynamics over time of the capital unemployment rate closely mirror those of the unemployment labor rate, a pattern consistent with standard intuition related to unemployment rates and with the findings depicted in Figure 1 of Ottonello (2021).

Figure A.2: Time Series of Capital Unemployment and Labor Rates



Note: Figure A.2 shows the time series of the capital unemployment rate and unemployment labor rate in the United Kingdom between 1990 and 2022. Labor unemployment data is obtained from ONS. The blue line represents the capital unemployment rate, whereas the dotted black line depicts the labor unemployment rate.

[26] See: ONS definitions.

A.3 More on The Spatial Persistence of Capital Unemployment Rates

Here, we present additional evidence on the persistence of capital unemployment rates in our data.

A.3.1 Additional Specifications. Figure A.3 displays binscatters of the capital unemployment rate against itself with 5- and 10-year lags, both with and without time fixed effects. The light blue circles represent group averages, while the dashed black line represents the 45-degree line.

Overall, we find that the binscatter group averages align closely with the 45-degree line, reaffirming the strong persistence of this variable. Additionally, we observe that controlling for time fixed effects does not significantly alter this result, suggesting that persistent nationwide shocks do not seem to drive the persistence. If anything, the persistence appears stronger after accounting for this.[27]

A.3.2 Evidence from Europe. In Section 2.2, we showed that capital unemployed rates exhibit significant persistence over time across UK cities. In this section of the Appendix, we assess the robustness of this finding by examining the persistence of this measure within European cities.

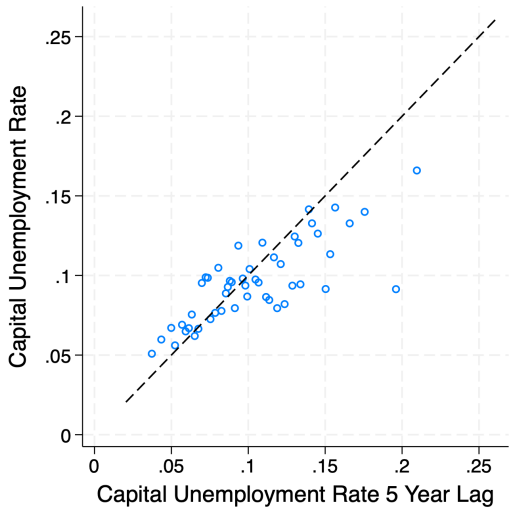
To assess the persistence of spatial differentials in the capital unemployment rate, we split the sample into two sub-periods: one before and the other after 2006. Figure A.4 plots the capital unemployment rate in the second subperiod against the capital unemployment rate in the first subperiod for every city in Europe. Notably, the capital unemployment rate across European cities also exhibits a high degree of persistence, aligning closely around the dashed black 45-degree reference line.

Overall, our findings suggest that persistence in the spatial distribution of capital unemployment rates seems to be a robust feature of local capital markets and does not appear to depend on the specific country of analysis.

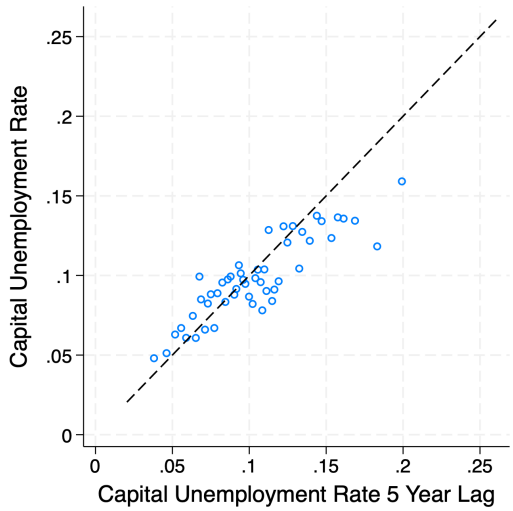
A.3.3 Accounting for Persistent Shocks. This section of the Appendix explores the potential role of persistent shocks in the documented persistence of capital unemployment rate gaps. These shocks may create a mismatch between the existing local supply of capital and the changing demand due to evolving local sectoral composition, driven by the deindustrial-

[27] Controlling for location-specific exposure to economy-wide industry cycles, as explained in Appendix A.3.3, yields very similar results, which are available upon request.

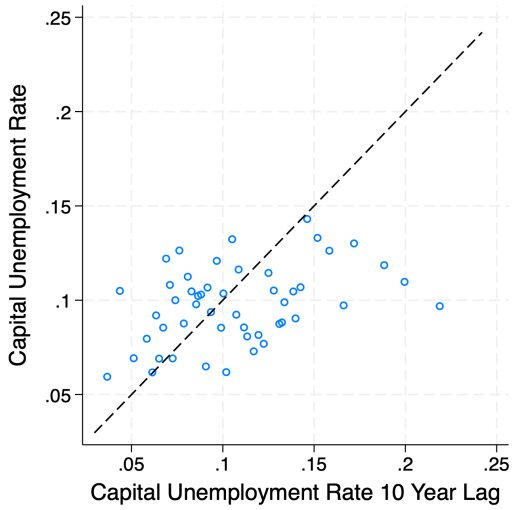
Figure A.3: Additional Evidence on the Persistence of Capital Unemployment Rate



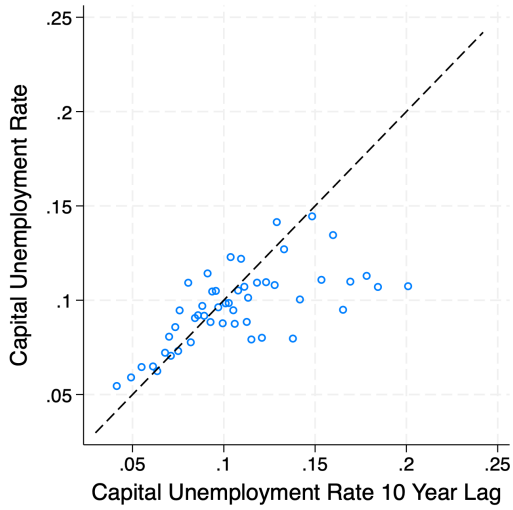
(a) 5-Year Lag without Time Fixed Effects



(b) 5-Year Lag with Time Fixed Effects



(c) 10-Year Lag without Time Fixed Effects



(d) 10-Year Lag with Time Fixed Effects

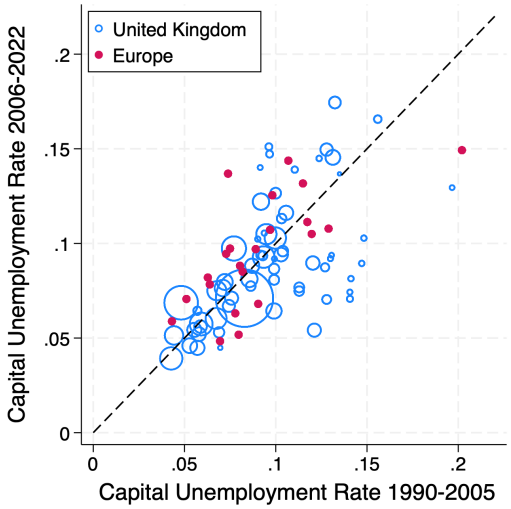
Note: Figure A.3 displays binscatters of the capital unemployment rate against itself with 5- and 10-year lags, both with and without time fixed effects. Light blue circles represent group averages. The dashed black line represents the 45-degree line.

ization process experienced by the UK.

To do so, we construct a location-specific exposure measure to economy-wide industry cycles. In particular, we define exposure as follows:

$$E_{jt-1990} = \sum_i \omega_{ij1990} \times \Delta_{t-1990} \log Y_{it}, \tag{41}$$

Figure A.4: Spatial Persistence of Capital Unemployment Rates in UK and Europe



(a) Persistence of Capital Unemployment Rate in UK and Europe

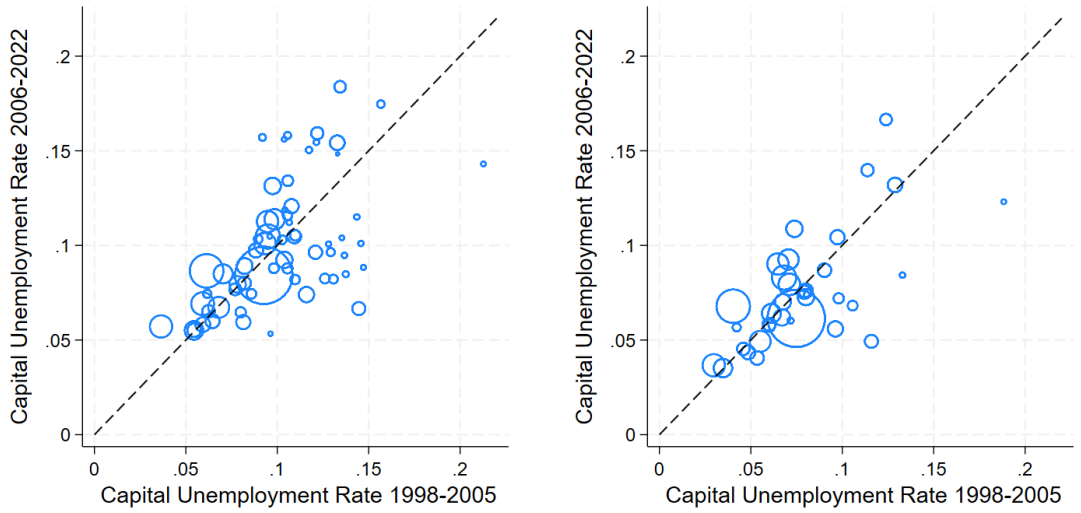
Note: Figure A.4 plots the capital unemployment rate in the UK and European cities in two subperiods of the sample. The blue open circles represent cities in the UK, and the size of each circle corresponds to the total capital within that city. The red circles represent cities in Europe. The dashed line represents the 45-degree line.

where i defines the industry, j the city, and t time. Thus, exposure is defined as the withed average, with weights given by the 1990 (initial) industry output share of total output in a given location, of cumulative changes since 1990 in industry output Y.

Figure A.5 plots capital unemployment rates in UK cities in two subperiods of the sample after controlling for time fixed effects (Figure A.5a) and time fixed effects and industry cycles simultaneously (Figure A.5b). The blue circles represent cities in the UK, and the size of each circle corresponds to the total capital within that city. The dashed line represents the 45-degree line. Overall, we find that accounting for time fixed effects and industry cycles does not significantly affect the persistent patterns documented in the main text. However, Figure A.5b is slightly less neat because controlling for industry cycles results in some loss of observations, as the PMA data define locations at a more granular level than the ONS. Thus, we conclude that while the UK economy has witnessed a slow-moving deindustrialization process, our data suggest that this is unlikely to be the main driver of the observed persistence in capital unemployment rates.

To reinforce this conclusion, we follow the approach used in Table 1 of the main text. Specifically, we regress the location-specific exposure measure to economy-wide industry

Figure A.5: Spatial Persistence Accounting for Persistent Shocks



(a) Without Time Fixed Effects

(b) Without Time Fixed Effects and Industry Cycles

Note: Figure A.5 plots capital unemployment rates in UK cities in two subperiods of the sample after controlling for time fixed effects (Figure A.5a) and time fixed effects and industry cycles simultaneously (Figure A.5b). The blue circles represent cities in the UK, and the size of each circle corresponds to the total capital within that city. The dashed line represents the 45-degree line.

cycles, as defined in equation (41), against the capital unemployment rate gaps. The results are presented in Table A.2.

Table A.2: Capital Unemployment Rate and Its Correlates

Dependent Variable	**Capital Unemployment Rate**	
	(1)	(2)
$E_{jt-1990}$	-0.02	-0.02
	(0.01)	(0.12)
Fixed Effects		
City	✗	✓
Time	✗	✓
Controls		
City-specific Time Trend	✗	✓
Observations	504	504

Note. City-specific time trends are quadratic. Standard errors are clustered at the city level and reported in parentheses. $^{+}$,*, **, and *** denote 15, 10, 5, and 1% statistical significance respectively.

Overall, we find that the location-specific exposure measure to economy-wide industry cycles has minimal and insignificant predictive power on capital unemployment rate gaps. This result confirms our previous findings from Figure A.5b and supports our conclusion that the UK deindustrialization process is unlikely to explain the capital unemployment rate gaps

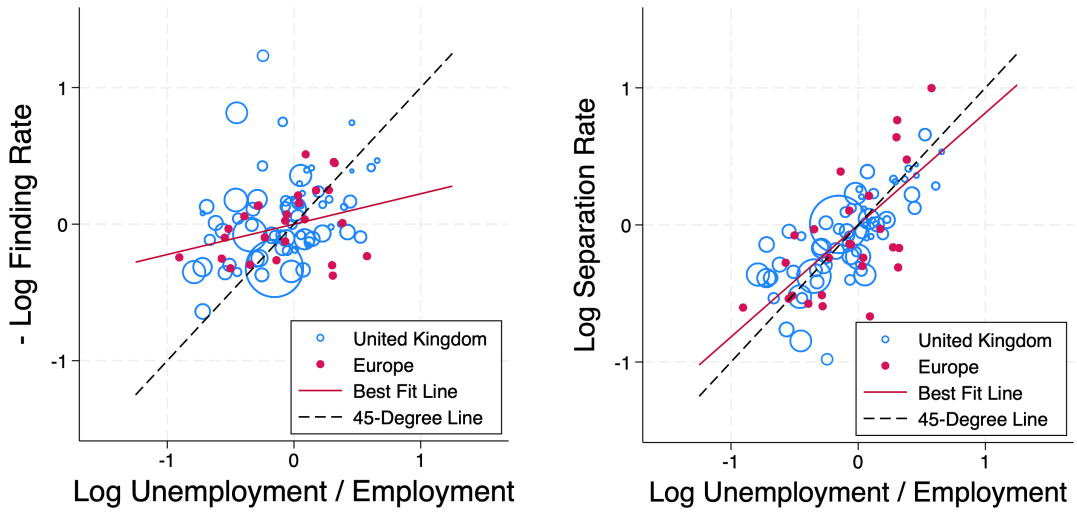
observed in the data.

A.4 More on The Spatial Ins and Outs of Unemployed Capital

Here, we present additional evidence on the central role of separation rates in explaining capital unemployment rate gaps in our data.

A.4.1 Descriptive Evidence for Europe. In this section of the Appendix, we assess whether the contributions of separation rates and finding rates to the local capital unemployment rate are comparable between UK and European cities.

Figure A.6: Capital Market Flows Across Space in UK and Europe



(a) Persistence of Total Capital **(b) Persistence of Unemployed Capital**

Note: Figure A.6 shows graphically the contribution of minus the log of the finding rate and the log of the separation rate to local capital unemployment rate differences across UK and European locations. Figure A.6a scatterplots minus the log of the finding rate against the log of the unemployment-employment capital ratio, across cities in the UK. Open blue circles represent cities in the UK, with size proportional to their total capital. Solid red circles represent cities in Europe. Each data point represents a within-city average, with cross-sectional means removed for the plot. The 45-degree line is in dashed black, and the line of best for European locations fit is in solid red. Figure A.6b scatterplots the log of the separation rate against the log of the unemployment-employment capital ratio, across cities in the UK and Europe.

Figure A.6 plots minus the log of finding rates f_j and the log of separation rates s_j against the log of the unemployment-employment capital rate ratio $\boldsymbol{k}_j^u/\boldsymbol{k}_j^e$ across cities in the UK (blue) and Europe (red). Figure A.6a suggests that finding rates exhibit relatively low variation across different locations, with the best-fit line notably distant from the 45-degree line (depicted in dashed black). In contrast, when examining separation rates, they emerge as the

primary factor driving differences in local capital unemployment rates. Figure A.6b shows that separation rates vary substantially across locations, with their best-fit line closely aligning with the 45-degree line.

Overall, our findings suggest that the quantitative importance of separation rates in explaining local capital unemployment rate differences seems to be a robust feature of local capital markets and does not seem to depend on the specific country we focus on.

A.4.2 Expanded Decompositions. In Section 3.1, we presented a decomposition of the log of the unemployment-employment capital rate ratio assuming $\delta \approx 0$. In this section of the Appendix, we instead present an expanded decomposition holding for any value of δ, assessing its impact on our empirical findings.

In particular, we can generalize equation (8) in the main text to the case with $\delta \neq 0$ yielding the following decomposition of the log of the unemployment-employment capital rate:

$$\log\left(\frac{\boldsymbol{k}_j^u}{\boldsymbol{k}_j^e}\right) = \log(s_j) - \log(f_j) + \log\left(\left(\frac{s_j(1-\delta) + (1-f_j)\delta/\boldsymbol{k}_j^e}{\delta + f_j(1-\delta)}\right)\frac{f_j}{s_j}\right). \tag{42}$$

The first two terms in equation (42) mirror those in equation (8), capturing the transitions in and out of the unemployment state for capital. The third term is new to this decomposition, specifically accounting for the extensive margin of unemployed capital associated with newly invested capital.

From equation (42), we arrive at a spatial decomposition of the variance of the log of the unemployment-employment capital rate ratio, given by:

$$\begin{aligned}\operatorname{Var}\left(\log\left(\frac{\boldsymbol{k}_j^u}{\boldsymbol{k}_j^e}\right)\right) = {} & \operatorname{Cov}\left(\log\left(\frac{\boldsymbol{k}_j^u}{\boldsymbol{k}_j^e}\right), \log(s_j)\right) + \operatorname{Cov}\left(\log\left(\frac{\boldsymbol{k}_j^u}{\boldsymbol{k}_j^e}\right), -\log(f_j)\right) \\ & + \operatorname{Cov}\left(\log\left(\frac{\boldsymbol{k}_j^u}{\boldsymbol{k}_j^e}\right), \log\left(\left(\frac{s_j(1-\delta) + (1-f_j)\delta/\boldsymbol{k}_j^e}{\delta + f_j(1-\delta)}\right)\frac{f_j}{s_j}\right)\right) \\ & + \operatorname{Cov}\left(\log\left(\frac{\boldsymbol{k}_j^u}{\boldsymbol{k}_j^e}\right), \varepsilon_j\right),\end{aligned} \tag{43}$$

where the last term can be calculated as the difference between the left-hand side and the first three terms of the decomposition, and is meant to capture measurement error in the data or departures from the steady-state assumption adopted in the analysis, as in the main text.

Thus, we can use equation (43) to inspect if our empirical findings from Section 3.2 are robust to allow for the extensive margin. Table A.3 presents the results from this expanded decomposition for the UK and Europe and compares them with the results from the decomposition outline by equation (9) in the main text.

Table A.3: Variance Decomposition of Local Unemployment-Employment Capital Ratio

	UK		Europe	
Direct flows: separation and finding rates (%)	98	98	104	104
Separation rate (%)	68	68	82	82
Finding rate (%)	30	30	22	22
Extensive margin due to investment (%)	–	-11	–	-10
Measurement error (%)	2	13	-4	6

Note: This table shows the variance decomposition of the log unemployment-employment capital ratio for the UK and Europe. Columns 2 and 4 show the variance decomposition in equation (9), while columns 3 and 5 show the variance decomposition in equation (43). Direct flows represent the contributions of separation and finding rates. All numbers are reported in percent.

We recover moderate values for measurement error, ranging from 2 to 13 percent, suggesting a modest role for measurement error or the the steady-state assumption adopted in the analysis. Additionally, we find that the extensive margin of unemployed capital accounts for approximately -11 percent in the UK and -10 percent in Europe. While the contribution of the extensive margin to changes in local unemployed capital is not zero, this augmented decomposition confirm that the predominant source of variation comes again from direct flows, with the separation rate playing a predominant quantitative role.

B Model Appendix

B.1 Rental Rate of Capital Derivation

Here we derive the rental rate of capital in equation (15). Using equations (12) and (14), we can rewrite the value of a firm producing as follows:

$$V_j^p(z) = y_j(z) - c - r_j(z) + \frac{\kappa}{q(\theta_j)}. \tag{44}$$

Nash bargaining implies the following first-order conditions: $(1-\eta)(V_j^e(z)-V_j^u)=\eta V_j^p(z)$. Thus, substituting equations (10), (11), and (44) into the Nash bargaining first-order conditions, we obtain the following expression:

$$(1-\eta)r_j(z)+\eta(1-f(\theta_j))\frac{\kappa}{q(\theta_j)}=\eta\left(y_j(z)-c-r_j(z)+\frac{\kappa}{q(\theta_j)}\right). \tag{45}$$

Using the property of the matching function such that $\frac{f(\theta_j)}{q(\theta_j)}=\theta_j$, we can rearrange the expression above and obtain the following:

$$r_j(z)=\eta\left(y_j(z)-c+\kappa\theta_j\right).$$

B.2 Tightness and Separation Cutoff Elasticities Derivations

Derivation of equation (20) *in Section 4.3.* Combining equations (14) and (16) we obtain the following:

$$\frac{\kappa}{q(\theta)}=(1-\delta)\beta(1-d)\mathbb{E}\left[(1-\eta)((y(z')-c)-\eta\kappa\theta+\frac{\kappa}{q(\theta)}\right]^+, \tag{46}$$

$$=(1-\delta)\beta(1-d)\left\{(1-F(z^R))\left[(1-\eta)(Z\mathbb{E}z'-c)-\eta\kappa\theta+\frac{\kappa}{q(\theta)}\right]\right\}, \tag{47}$$

Which can be rearranged as follows:

$$\eta A(1-F(z^R))\theta+\frac{1-A(1-F(z^R))}{q(\theta)}=\frac{1-\eta}{\kappa}A(1-F(z^R))(Z\mathbb{E}z'-c), \tag{48}$$

where $A\equiv(1-\delta)\beta(1-d)$. After implicit differentiating the LHS of equation (48) with respect to Z the following is obtained:

$$\left(\eta A(1-F(z^R))+\frac{(1-A(1-F(z^R))\varepsilon_{q,\theta}}{\theta q(\theta)}\right)\frac{\partial\theta}{\partial Z}+A\left(\eta\theta-\frac{1}{q(\theta)}\right)\frac{\partial(1-F(z^R))}{\partial z^R}\frac{\partial z^R}{\partial Z}. \tag{49}$$

While implicitly differentiating the RHS of equation (48) with respect to Z the following is obtained:

$$\frac{(1-\eta)A(1-F(z^R))}{\kappa}\left(\mathbb{E}z' + Z\frac{\partial \mathbb{E}z'}{\partial z^R}\frac{\partial z^R}{\partial Z} + \frac{Z\mathbb{E}z'-c}{1-F(z^R)}\frac{\partial(1-F(z^R))}{\partial z^R}\frac{\partial z^R}{\partial Z}\right). \tag{50}$$

Equating (49) and (50) and rearranging we obtain the following:

$$\begin{aligned}\frac{\partial\theta}{\partial Z} &= \frac{\theta q(\theta)}{\eta A(1-F(z^R))\theta q(\theta) + (1-A(1-F(z^R))\varepsilon_{q,\theta}}\frac{(1-\eta)A(1-F(z^R))}{\kappa} \\ &\times\left(\mathbb{E}z' + Z\frac{\partial \mathbb{E}z'}{\partial z^R}\frac{\partial z^R}{\partial Z} + \frac{Z\mathbb{E}z'-c}{1-F(z^R)}\frac{\partial(1-F(z^R))}{\partial z^R}\frac{\partial z^R}{\partial Z}\right) \\ &- \frac{\theta q(\theta)}{\eta A(1-F(z^R))\theta q(\theta) + (1-A(1-F(z^R))\varepsilon_{q,\theta}}A\left(\eta\theta - \frac{1}{q(\theta)}\right)\frac{\partial(1-F(z^R))}{\partial z^R}\frac{\partial z^R}{\partial Z}.\end{aligned} \tag{51}$$

Using the following relation:

$$\frac{\theta q(\theta)}{\eta A(1-F(z^R))\theta q(\theta) + (1-A(1-F(z^R))\varepsilon_{q,\theta}}\frac{(1-\eta)A(1-F(z^R))}{\kappa} = \Upsilon\frac{\theta}{Z\mathbb{E}z'-c}, \tag{52}$$

where $\Upsilon \equiv \frac{\eta A(1-F(z^R))\theta q(\theta)+(1-A(1-F(z^R)))}{\eta A(1-F(z^R))\theta q(\theta)+(1-A(1-F(z^R))\varepsilon_{q,\theta}}$, we get the following:

$$\begin{aligned}\frac{\partial\theta}{\partial Z} &= \Upsilon\frac{\theta}{Z\mathbb{E}z'-c}\left(\mathbb{E}z' + Z\frac{\partial \mathbb{E}z'}{\partial z^R}\frac{\partial z^R}{\partial Z} + \frac{Z\mathbb{E}z'-c}{1-F(z^R)}\frac{\partial(1-F(z^R))}{\partial z^R}\frac{\partial z^R}{\partial Z}\right) \\ &- \frac{\theta q(\theta)}{\eta A(1-F(z^R))\theta q(\theta) + (1-A(1-F(z^R))\varepsilon_{q,\theta}}A\left(\eta\theta - \frac{1}{q(\theta)}\right)\frac{\partial(1-F(z^R))}{\partial z^R}\frac{\partial z^R}{\partial Z}.\end{aligned} \tag{53}$$

Rearranging and partial derivatives in terms of elasticities we obtain the following:

$$\varepsilon_{\theta,Z} = \Upsilon\frac{\mathbb{E}y(z')}{\mathbb{E}y(z')-c} + \Upsilon\frac{\mathbb{E}y(z')}{\mathbb{E}y(z')-c}\Omega\varepsilon_{z^R,Z}, \tag{54}$$

where

$$\Omega \equiv \varepsilon_{\mathbb{E}z',z^R} + \frac{\mathbb{E}y(z')-c}{\mathbb{E}y(z')}\left(1 + \frac{\kappa(1-\eta p(\theta))}{q(\theta)(1-\eta)(\mathbb{E}y(z')-c)}\right)\varepsilon_{1-F(z^R),z^R}. \tag{55}$$

Derivation of equation (23) *in Section 4.3.* The separation threshold level z^R is implicitly

defined by equation (17) and can be rearranged as follows:

$$z^R = \frac{1}{Z}\left(c + \frac{\eta}{1-\eta}\kappa\theta - \frac{\kappa}{1-\eta}\frac{1}{q(\theta)}\right). \tag{56}$$

Differentiating it with respect to Z and rearranging it yields the following expressions:

$$\frac{\partial z^R}{\partial Z} = \underbrace{-\frac{1}{Z^2}\left(c + \frac{\eta}{1-\eta}\kappa\theta - \frac{\kappa}{1-\eta}\frac{1}{q(\theta)}\right)}_{\text{part 1}} + \underbrace{\frac{1}{Z}\left(\frac{\eta}{1-\eta} + \frac{1}{1-\eta}\frac{1}{q(\theta)^2}q'(\theta)\right)\kappa\frac{\partial\theta}{\partial Z}}_{\text{part 2}}. \tag{57}$$

Substituting equation (56) in part 1 of (57) we get the following:

$$\frac{\partial z^R}{\partial Z} = -\frac{1}{Z}\left(\frac{\kappa}{1-\eta}\left(-\frac{q'(\theta)}{q(\theta)^2} - \eta\right)\frac{\partial\theta}{\partial Z} + z^R\right),$$

which can be re-expressed in terms of elasticities as follows:

$$\varepsilon_{z^R,Z} = -1 - \frac{\kappa\theta}{(1-\eta)y(z^R)}\left(\frac{\varepsilon_{q,\theta}}{p(\theta)} - \eta\right)\varepsilon_{\theta,Z}.$$

B.3 Social Planner Derivations

This section of the Appendix derives the first-order conditions of the social planner's problem characterized by equations (25) and (26) in Section 4.5. Here, $\mathbb{E}z_j$ is given by the following expression:

$$\mathbb{E}z_j = \frac{1}{1-F(z_j^R)}\int_{z_j^R}^{z_j^{\max}} z_j f(z_j) dz_j.$$

The first-order condition with respect to v_j is given by the following expression:

$$\kappa = -\beta(1-\delta)q(\theta_j)(1-d)(1-\varepsilon_{q_j,\theta_j})(1-F(z_j^R))\frac{\partial\omega'}{\partial k_j^{u'}}, \tag{58}$$

where we adopt the notation $\omega' \equiv \omega(k_j^{u'}, y_j')$ for conciseness. Rearranging equation (58) we obtain the following:

$$\kappa = (1-\delta)\beta q(\theta_j)(1-d)\mathbb{E}\left[V_j^{p,SP}(z')\right]^+, \tag{59}$$

where $\mathbb{E}V_j^{p,SP}(z') \equiv -(1-\varepsilon_{q_j,\theta_j})\frac{\partial\omega'}{\partial k_j^{u'}}$, as explained in the main text. Moreover, by rearranging the forwarded envelope condition we obtain the following:

$$\frac{\partial\omega'_j}{\partial k_j^{u'}} = c - \mathbb{E}y_j(z) - \frac{\kappa}{q(\theta_j)}\frac{1}{1-\varepsilon_{q_j,\theta_j}}(1-\varepsilon_{q_j,\theta_j}p(\theta_j)), \tag{60}$$

which can be rearranged as follows:

$$\mathbb{E}V_j^{p,SP}(z) = (1-\varepsilon_{q,\theta})\left(\mathbb{E}y_j(z) - c\right) - \varepsilon_{q,\theta}\kappa\theta_j + \frac{\kappa}{q(\theta_j)}. \tag{61}$$

The first-order condition with respect to z_j^R is given by the following:

$$\frac{\partial\omega'_j}{\partial k_j^{u'}}\frac{\partial k_j^{u'}}{\partial z_j^R} + \frac{\partial\omega'_j}{\partial\mathbb{E}y_j(z')}Z_j\frac{\partial\mathbb{E}z_j}{\partial z_j^R} = 0, \tag{62}$$

where:

$$\frac{\partial k_j^{u'}}{\partial z_j^R} = -k_j^{u'}p(\theta_j)(1-\delta)(1-d)\frac{\partial(1-F(z_j^R))}{\partial z_j^R} - (1-k_j^{u'})(1-\delta)(1-d)\frac{\partial(1-F(z_j^R))}{\partial z_j^R}, \tag{63}$$

$$\frac{\partial\omega'_j}{\partial\mathbb{E}y'_j} = 1 - k_j^{u'}. \tag{64}$$

Substitute equations (60), (63) (64) into equation (62) we obtain the following:

$$\begin{aligned} 0 = &\left(c - \mathbb{E}y_j(z) - \frac{\kappa}{p'(\theta_j)}(1-\varepsilon_{q_j,\theta_j}p(\theta_j))\right) \\ &\times\left(-k_j^{u'}p(\theta_j) - (1-k_j^{u'})\right)(1-\delta)(1-d)\frac{\partial(1-F(z_j^R))}{\partial z_j^R} \\ &+ (1-k_j^{u'})Z_j\frac{\partial\mathbb{E}z_j}{\partial z_j^R}\frac{(1-F(z_j^R))}{\frac{\partial(1-F(z_j^R))}{\partial z_j^R}}. \end{aligned}$$

After substituting in the law of motion of capital, the above equation can be written as follows:

$$\left(c - \mathbb{E}y_j(z) - \frac{\kappa}{p'(\theta_j)}(1-\varepsilon_{q_j,\theta_j}p(\theta_j))\right) + Z_j\frac{\partial\mathbb{E}z_j}{\partial z_j^R}\frac{(1-F(z_j^R))}{\frac{\partial(1-F(z_j^R))}{\partial z_j^R}} = 0. \tag{65}$$

Using Leibniz integral rule, the term $\frac{\partial \mathbb{E}z_j}{\partial z_j^R}$ can be calculated as follows:

$$\frac{\partial \mathbb{E}z_j}{\partial z_j^R} = \frac{1}{1 - F(z_j^R)} \left[\frac{\partial (1 - F(z_j^R))}{\partial z_j^R} (z_j^R - \mathbb{E}z_j) \right]. \tag{66}$$

Thus, substituting equation (66) into equation (65) yields the following:

$$0 = (1 - \varepsilon_{q,\theta}) \left(y_j(z_j^R) - c \right) - \varepsilon_{q,\theta} \kappa \theta_j + \frac{\kappa}{q(\theta_j)}. \tag{67}$$

C Quantitative Appendix

C.1 Amenities

Here, we correlate the estimated amenities with an amenity score provided by PMA, as well as with ONS data on the location's average distance from a train station, airport, and hospital. We standardize all variables to ensure comparability of units. Table C.4 shows the results. Overall, higher amenity score is positively associated with higher estimated amenities, while larger distances from a train station, airport, and hospital are associated with lower estimated amenities.

Table C.4: Correlation of Estimated Amenities with Observables

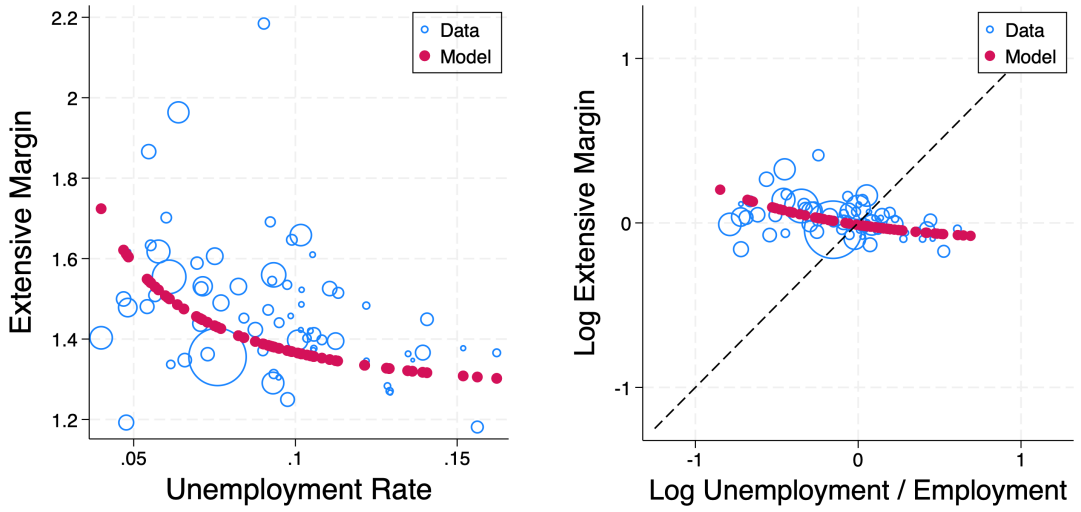
Dependent Variable	**Amenities**
Amenity index	0.71
	(0.65)
Distance from	
train station	-1.24*
	(0.62)
airport	-0.41
	(0.41)
hospital	-1.41**
	(0.69)
Observations	34
R^2	0.71

Note. All variables are standardized to ensure comparability of units. Observation are weighted by location relative size. Robust standard errors are reported in parentheses. $^+$,*, **, and *** denote 15, 10, 5, and 1% statistical significance respectively.

C.2 Extensive Margin

In this section, we compare the contribution of the extensive margin to spatial capital unemployment rate differences in the model and the data.

Figure C.7: Extensive Margin and Capital Unemployment Gap Differences



(a) Raw Data **(b) Contribution to Decomposition (43)**

Note: Figure C.7 illustrates the extensive margin and its contribution to local capital unemployment rate differences in the model (blue) and data (red), across UK locations. In Figure C.7a, the extensive margin is plotted against the local unemployment rate, along with the dashed black 45-degree line. Figure C.7b displays the demeaned log of the extensive margin against the demeaned log of the unemployment-employment capital ratio, also with the dashed black 45-degree line. The size of the circles is proportional to the size of the location.

Figure C.7 presents our results related to the extensive margin. Figure C.7a shows the extensive margin across locations with different capital unemployment rates both in the data (blue) and the model (red). The model captures well both the decline of the extensive margin with the capital unemployment rate as well as its quantitative magnitude. We recall that none of this has been targeted in our calibration strategy, making it a successful result of the model. Figure C.7b displays the demeaned log of the extensive margin against the demeaned log of the unemployment-employment capital ratio both in the data (blue) and the model (red), as required by the augmented decomposition (43) in Appendix A.4.2.

Table C.5 compares the variance decomposition of log unemployment-employment capital ratio between data and model. Columns 1 and 3 show the variance decomposition in equation (9) in the model and the data as discussed in the main text, while columns 2 and 4 show the variance decomposition in equation (43) without measurement error in the model

Table C.5: Variance Decomposition of Local Unemployment-Employment Capital Ratio

	Data		Model	
Direct flows: separation and finding rates (%)	100	112	100	117
Separation rate (%)	69	78	68	79
Finding rate (%)	31	34	32	38
Extensive margin due to investment (%)	–	-12	–	-17

Note: This table compares the variance decomposition of log unemployment-employment capital ratio between data and model. Columns 1 and 3 show the variance decomposition in equation (9), while columns 2 and 4 show the variance decomposition in equation (43) without measurement error. Direct flows represent the contributions of separation and finding rates. All numbers are reported in percent.

and the data. The model captures well quantitatively the major contribution of the separation rate and the minor one of the finding rate, as well as the negative contribution of the extensive margin.